



# Experimental microkinetic approach of the CO/H<sub>2</sub> reaction on Pt/Al<sub>2</sub>O<sub>3</sub> using the Temkin formalism. 2. Coverages of the adsorbed CO and hydrogen species during the reaction and rate of the CH<sub>4</sub> production



Julien Couble, Daniel Bianchi \*

Institut de Recherche sur la Catalyse et l'Environnement de Lyon (IRCELYON), UMR 5256 CNRS, Université Claude Bernard Lyon 1, Bat. Chevreul, 43 Boulevard du 11 Novembre 1918, 69622 Villeurbanne, France

## ARTICLE INFO

*Article history:*  
Received 1 March 2017  
Revised 2 May 2017  
Accepted 18 May 2017  
Available online 23 June 2017

*Keywords:*  
Experimental microkinetic  
Pt/Al<sub>2</sub>O<sub>3</sub>  
CO/H<sub>2</sub> reaction  
FTIR spectroscopy  
Temkin formalism

## ABSTRACT

The present experimental microkinetic approach is dedicated to the interpretation using the Temkin formalism of the experimental evolutions of (a) the coverage of adsorbed CO and hydrogen species and (b) the rate of the CH<sub>4</sub> production during the increase in the temperature for x% CO/H<sub>2</sub> gas mixtures ( $x = 1, 10^{-2}$  and  $10^{-3}$ , P<sub>T</sub> = 1 atm) on a reduced 2.9% Pt/Al<sub>2</sub>O<sub>3</sub> catalyst (Pt dispersion D ≈ 0.26). FTIR spectroscopy (a) shows that three adsorbed CO species: linear, bridged and threefold coordinated CO species (denoted L, B and 3FC respectively) are formed at 300 K and (b) provides the evolution of the coverage of the dominant L CO species (IR band at 2080 cm<sup>-1</sup> at 300 K) for the three CO/H<sub>2</sub> gas mixtures in the 300–740 K temperature range. These data support the development of a rigorous (without approximations) competitive adsorption model associated with a reaction based on the Temkin formalism (denoted Temkin-C.R model). This model provides (a) the theoretical coverages of the L CO and hydrogen species and (b) the theoretical rate of the CH<sub>4</sub> production during the CO/H<sub>2</sub> reaction as a function of the partial pressures of the reactants and the reaction temperature which are compared to the experimental data. This shows that the L CO species which dominates the CO adsorption is not the active adsorbed species at the beginning of the CH<sub>4</sub> production (T ≈ 475 K for 1% CO/H<sub>2</sub>). It is shown that the active species is the 3FC CO species which represents ≈ 1/7 of the total amount of adsorbed CO species. These conclusions are consistent with literature data on Pt particles indicating that a small number of sites/adsorbed CO species are involved at the beginning of the CO/H<sub>2</sub> reaction. Moreover, as a contribution to the debate on the paradox of kinetics on heterogeneous surfaces, the Temkin-C.R model is compared to models based on the Langmuir formalism mainly used in kinetic studies. This reveals the clear advantage of the Temkin-C.R model for the representation of experimental data in large ranges of experimental conditions.

© 2017 Elsevier Inc. All rights reserved.

## 1. Introduction

The present study (Parts 1 [1] and 2) is dedicated to the development of an experimental microkinetic approach (denoted EMA) of the CO/H<sub>2</sub> reaction at atmospheric total pressure (mainly CH<sub>4</sub> formation) on a 2.9% Pt/Al<sub>2</sub>O<sub>3</sub> catalyst. The EMA consists measuring by experimental procedures the kinetic parameters of the surface elementary steps (i.e. coverages of the adsorbed species, heats of adsorption, activation energies) of a plausible kinetic model of a gas/solid heterogeneous catalytic reaction for the comparison between the experimental and theoretical rates of the reaction (Ref. [1] and references therein). It has been shown by FTIR spec-

troscopy that the adsorption of x% CO/H<sub>2</sub> ( $x = 1, 10^{-2}$  and  $10^{-3}$ ) at 300 K on 2.9% Pt/Al<sub>2</sub>O<sub>3</sub> leads to the formation on the Pt particles of (a) mainly linear CO species and (b) small amounts of bridged and threefold coordinated CO species (denoted L, B and 3FC CO species respectively) [1]. The evolutions of the intensity of the IR band of the L CO species with the increase in the temperature T (in the 300–713 K range) in the presence of the three x% CO/H<sub>2</sub> gas mixtures (in parallel to the CH<sub>4</sub> production for T > 475 K for  $x = 1$ ) have been used to determine the change in the coverage of the L CO species with T:  $\theta_L^{Exp} = f(T)$  [1]. It has been shown that the three experimental curves  $\theta_L^{Exp} = f(T)$  are consistent with a competitive chemisorption model between the L CO and hydrogen species according to the Temkin formalism (denoted Temkin-C model) in large range of temperatures: 300–713 K, 300–610 K and 300–520 K for  $x = 1, 10^{-2}$  and  $10^{-3}$  respectively. The Temkin-C model

\* Corresponding author.

E-mail address: [daniel.bianchi@ircelyon.univ-lyon1.fr](mailto:daniel.bianchi@ircelyon.univ-lyon1.fr) (D. Bianchi).

overestimates the coverage of the L CO species as compared to the experimental data for  $T > 610$  K and  $T > 520$  K for  $x = 10^{-2}$  and  $10^{-3}$  respectively. This has been qualitatively ascribed to the perturbation (for  $x < 1$ ) of the competitive adsorption equilibrium between the adsorbed L CO and hydrogen species by the surface elementary steps implicated in the CH<sub>4</sub> production [1]. In the present Part 2, the Temkin-C model is developed to take into account the impact of these perturbations leading to a model for competitive adsorption model with reaction (denoted Temkin-C.R). This model provides (a) the theoretical evolutions of the coverages of the L CO and hydrogen species consistent with the experimental data in temperature range 300–713 K for the three  $x\%$  CO/H<sub>2</sub> gas mixtures and (b) the theoretical rate (in TOF (s<sup>-1</sup>)) of the CH<sub>4</sub> production at low CO conversions (<15%) for  $x = 1$  considering a reaction between the L CO and hydrogen adsorbed species which is compared to the experimental rate. The Temkin-C and Temkin-C.R models constitute an extension of the Temkin adsorption model [2] which has been used in previous studies for the determination in the absence of competition of the individual heats of adsorption at high and low coverages of (a) the L, B and 3FC CO species [3–10] and (b) the hydrogen species [11] on 2.9% Pt/Al<sub>2</sub>O<sub>3</sub>.

## 2. Experimental

The experimental conditions are identical to those described in detail in Part 1 [1] and they are briefly summarized to facilitate the presentation.

### 2.1. Catalyst and characterization

The 2.9% Pt/Al<sub>2</sub>O<sub>3</sub> (in wt.%, alumina from Degussa, 100 m<sup>2</sup>/g, incipient wetness method, aqueous solution of H<sub>2</sub>PtCl<sub>6</sub> × H<sub>2</sub>O) was reduced in hydrogen on the different set-ups as follows: He (300 K) → He (5 K/min, 713 K for 10 min) → O<sub>2</sub> (713 K, 10 min) → He (713 K, 10 min) → H<sub>2</sub> (713 K, 30 min) → He (713 K, 5 min) → He (300 K). In some experiments the solid was cooled to 300 K in hydrogen. In Part 1 [1], the experiments have been performed for two Pt dispersions:  $D \approx 0.6$  and 0.26 obtained by ageing procedures from the fresh solid ( $D = 0.84$ ). In the present study the solid with  $D \approx 0.26$  has been used because it is favorable to the repeatability of the experiments on the same sample.

### 2.2. IR cell reactor

A small pathlength ( $\approx 2$  mm) home made stainless steel IR cell in transmission mode with CaF<sub>2</sub> windows [12] using compressed disks of solid ( $\Phi = 1.8$  cm,  $m \approx 40$ –80 mg) has been used. The adsorbed species can be studied in the temperature range of 293–800 K with a controlled gas flow rate in the range of 150–2000 cm<sup>3</sup> min<sup>-1</sup> at atmospheric pressure selected using different valves and purified by different traps in particular cold traps for H<sub>2</sub>O impurities (77 K using helium and CO/H<sub>2</sub> gas mixtures).

### 2.3. Volumetric measurements using mass spectrometry

An analytical system for transient experiments has been used to quantify (a) the amounts of adsorbed CO and H<sub>2</sub> species at 300 K on the 2.9% Pt/Al<sub>2</sub>O<sub>3</sub> solid and (b) the rate of the CH<sub>4</sub> production from the hydrogenation of CO during the increase in  $T$  (light-off tests). Briefly, the composition (molar fractions  $X_i$ ) of the gas mixture at the outlet of a quartz micro reactor containing the pre-treated catalyst (weight range of 0.05–0.5 g, deposited on quartz wool, (see Part [1] for others characteristics of the solid sample and reactor) was determined, by using a quadrupole mass spectrometer during either switches between regulated gas flows

(1 atm, flow rate in the 100–500 cm<sup>3</sup> min<sup>-1</sup> range) at a constant temperature or an increase in the temperature (measured via a stainless steel  $K$  type thermocouple:  $\Phi = 0.25$  mm) using a furnace of low thermal inertia [1]. The molar fractions provided the evolution with time on stream  $t$  of the rates of either formation of a product  $j$ :  $R_j(t) = X_j(t) M_F/m_C$  or consumption of a reactant  $i$ :  $R_i(t) = (X_{in} - X_i(t)) M_F/m_C$  where  $M_F$  and  $m_C$  were the total molar flow rate and the weight of catalyst respectively and  $X_{in}$  was the molar fraction at the inlet of the reactor. The integration of the rates with time on stream provided the amounts of gaseous species either consumed or produced in μmol/g of catalyst during the experiments.

### 2.4. Competitive chemisorption between CO and H<sub>2</sub> and CO hydrogenation on 2.9% Pt/Al<sub>2</sub>O<sub>3</sub>

The experimental procedures on the FTIR and M.S setups were as follows:

#### 2.4.1. FTIR setup

After the reduction of the solid in H<sub>2</sub> at 713 K, it was cooled in H<sub>2</sub> to 300 K and then a 1% CO/H<sub>2</sub> mixture was introduced. After the steady state, the temperature was increased ( $\approx 10$  K/min) to 713 K followed by a cooling stage to 300 K in the presence of 1% CO/H<sub>2</sub> whereas the FTIR spectra of the adsorbed species were recorded periodically. After a switch 1% CO/H<sub>2</sub> → 10<sup>-2</sup>% CO/H<sub>2</sub> at 300 K, similar experiments have been performed. These experiments have been repeated for 10<sup>-3</sup>% CO/H<sub>2</sub> after the following series of switches at 300 K: 10<sup>-2</sup>% CO/H<sub>2</sub> → 1% CO/H<sub>2</sub> → 10<sup>-3</sup>% CO/H<sub>2</sub>.

#### 2.4.2. M.S setup

After the reduction of the solid (mass of catalyst 0.098 g) in H<sub>2</sub> at 713 K it was cooled in helium to 300 K. Then after the switch He → 1% CO/1% Ar/He to quantify the total amount of adsorbed CO species ( $Q_{CO}(300\text{ K}) = 48$  μmol/g) (see [1] for more details), a switch 1% CO/1% Ar/He → 1% CO/1% Ar/H<sub>2</sub> was performed and then the temperature was increased ( $\approx 0.3$  K/s) to 713 K. This provided the evolution of the rate of the CH<sub>4</sub> production:  $R_{CH_4}$  in μmol (g of catalyst)<sup>-1</sup> s<sup>-1</sup> and then the turnover frequency by considering that  $Q_{CO}(300\text{ K})$  quantified the amount of Pt sites active during CO/H<sub>2</sub> reaction:  $TOF_{CH_4} = R_{CH_4}/Q_{CO}(300\text{ K})$  in s<sup>-1</sup>.

## 3. Result and discussion

The main experimental data linked to the CH<sub>4</sub> production from the CO/H<sub>2</sub> reaction on 2.9% Pt/Al<sub>2</sub>O<sub>3</sub> have been described in detail in Part 1 [1]. Some of them are briefly presented to facilitate the presentation of the Temkin-C.R model.

### 3.1. FTIR study of the CO-H<sub>2</sub> chemisorption on 2.9% Pt/Al<sub>2</sub>O<sub>3</sub>

The adsorption of 1% CO/H<sub>2</sub> at 300 K on the reduced 2.9% Pt/Al<sub>2</sub>O<sub>3</sub> solid for  $D \approx 0.26$  leads to the detection of three IR bands (inset Fig. 1) at 2080 cm<sup>-1</sup> (very strong), 1835 cm<sup>-1</sup> (weak) and 1780 cm<sup>-1</sup> (weak) indicating the formation of three adsorbed CO species: linear (which dominates the CO adsorption), bridged and three fold coordinated respectively ([1] and references therein). These IR bands are similar to those observed using 1% CO/He [3–5]. The strong IR band of the L CO species explains that the present EMA is dedicated to its role during the CO/H<sub>2</sub> reaction. Fig. 1 shows the evolution of the IR band of the L CO species on 2.9% Pt/Al<sub>2</sub>O<sub>3</sub> catalyst during the increase in  $T$  for 1% CO/H<sub>2</sub> after a first heating to 713 K/cooling to 300 K cycles to obtain reproducible IR spectra [1]. It can be observed that, in the range of 373–473 K (spectra a and b in Fig. 1), the IR band of the L CO species shifts to lower

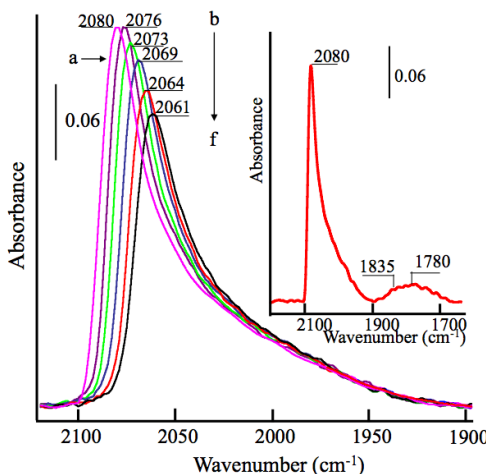


**Fig. 1.** Evolution of the IR band of the LCO species for 1% CO/H<sub>2</sub> on the reduced 2.9% Pt/Al<sub>2</sub>O<sub>3</sub> solid ( $D = 0.26$ ) as a function of the temperature: (a)–(f)  $T = 373, 473, 553, 643, 696$  and 715 K. Inset: IR bands of the different adsorbed CO species formed at 300 K for 1% CO/H<sub>2</sub> on the freshly reduced solid.

wavenumbers (2082–2076 cm<sup>-1</sup>) whereas its intensity remains unchanged. For  $T > 573$  K the IR band decreases progressively associated with a shift to lower wavenumbers (2061 cm<sup>-1</sup> at 715 K) consistent with a decrease in the coverage of the L CO species.

The data in Fig. 1 are similar to those observed in previous studies with 1% CO/He on the same catalyst [3–5]. Experiments similar to Fig. 1 have been performed with 10<sup>-2</sup>% and 10<sup>-3</sup>% CO/H<sub>2</sub> [1].

### 3.2. Experimental evolution of the coverage of the L CO species

According to the AEIR method [3–10] the IR spectra in Fig. 1 provide the evolution of the coverage of the L CO species according to:

$$\theta_L(T_a) = \frac{Q_L}{Q_{Lsat}} = \frac{A_L(T_a)}{A_L(M)} \quad (1)$$

where  $Q_L$  ( $A_L(T_a)$ ) and  $Q_{Lsat}$  ( $A_L(M)$ ) are the amounts (area in the absorbance mode of the IR band) of the L CO species at  $T_a$  and at saturation of the sites respectively. The saturation of the sites is attested by showing that the intensity of the IR band is independent on the adsorption pressure at low temperatures (i.e. inset of Fig. 2A for the IR band of the L CO species at 300 K for  $P_{CO} = 1000$  and 1 Pa). Eq. (1) considers a linear relationship between  $Q_L$  and  $A_L(T_a)$  which has been attested previously [13] as for others adsorbed species on different solids [14–16].

Eq. (1) and the data in Fig. 1 provide symbols  $\circ$  in Fig. 2A which give  $\theta_L^{Exp}(T_a)$ , the experimental evolution of the coverage of the L CO species in the presence of 1% CO/H<sub>2</sub> on 2.9% Pt/Al<sub>2</sub>O<sub>3</sub> for  $D \approx 0.26$ .

Experiments similar to Fig. 1 have been performed with 10<sup>-2</sup>% CO/H<sub>2</sub> and 10<sup>-3</sup>% CO/H<sub>2</sub> providing symbols  $\square$  and  $\Delta$  in Fig. 2A respectively. The same experimental evolutions of  $\theta_L^{Exp}(T_a)$  has been observed for  $D = 0.6$  [1] showing that they are not strongly dependent on  $D$ .

Curves a, b, and c in Fig. 2A give the theoretical evolutions of the coverage of the L CO species:  $\theta_L^{Th.}(T_a)$  from the Temkin-C model [1] for  $x = 1, 10^{-2}$  and  $10^{-3}$  respectively using the heats of adsorption of the L CO and hydrogen species determined in previous works in the absence of competition (see Table 1) [3–5,11]. For 1% CO/H<sub>2</sub>, curve a in Fig. 2A shows that  $\theta_L^{Th.}(T_a)$  overlaps  $\theta_L^{Exp.}(T_a)$  in the temperature range of 300–713 K whereas for 10<sup>-2</sup>% CO/H<sub>2</sub> and 10<sup>-3</sup>%

CO/H<sub>2</sub>, the  $\theta_L^{Th.}(T_a)$  curves (b and c) overestimate the experimental data (symbols  $\square$  and  $\Delta$  respectively) for  $T > 640$  K and  $T > 520$  K respectively. These situations have been qualitatively explained considering that, at high temperatures, the surface elementary steps implicated in the CH<sub>4</sub> formation disturb (for  $x = 10^{-2}$  and  $10^{-3}$ ) or not (for  $x = 1$ ) the competitive L CO-H<sub>2</sub> adsorption equilibrium. The aim of the present study is to develop the Temkin-C model [1] by considering the elementary steps of the CH<sub>4</sub> production to obtain theoretical curves consistent with the experimental data in the full temperature range for the three  $x\%$  CO/H<sub>2</sub> gas mixtures. Moreover, similarly to Part 1 [1] to demonstrate the interest of the Temkin formalism a comparison is presented considering (a) the Langmuir formalism which is classically used in many kinetic studies of gas/solid heterogeneous catalysis and (b) a pseudo Langmuir formalism based on a mathematical approximation of the Langmuir model at a macroscopic level.

### 3.3. On the EMA of the CO/H<sub>2</sub> reaction considering the L CO species as active species

It is well known [17–20] that CO/H<sub>2</sub> gas mixtures on Pt/Al<sub>2</sub>O<sub>3</sub> catalysts, at  $T > \approx 500$  K, lead to the production of CH<sub>4</sub> ( $\approx 96\%$  whatever the H<sub>2</sub>/CO ratio in the 0.5–10 range) [17] which can be associated with small amounts of C<sub>2</sub> species [17] and oxygenated species [19]. In particular Panagiotopoulou et al. [20] using a 0.5 wt% NM/Al<sub>2</sub>O<sub>3</sub> (NM = Ru, Rh, Pt and Pd) with a reactive mixture similar to the present study: 1% CO/50% H<sub>2</sub>/He, show from light-off tests that the Pt containing solid ( $D = 1$ ) is one of the less active catalyst with a CH<sub>4</sub> production starting at  $\approx 523$  K as compared to  $\approx 473$  K for the best catalysts (Ru and Rh). The experimental kinetic approach of the reaction at low conversions (<5% of CO) for  $T = 548$  K assuming that the rate for methanation is:  $N_{CH_4} = A \exp(-E_m/RT) P_{H_2}^X P_{CO}^Y$  has shown that X and Y are close to 1 and 0 suggesting that the surface is mainly covered of adsorbed CO species due to a favorable competitive adsorption of CO with hydrogen [17,18]. This was confirmed by an FTIR study [21] on Pt/SiO<sub>2</sub>-Al<sub>2</sub>O<sub>3</sub> showing that, at  $T = 548$  K, there are no significant differences in the intensity of the IR band of the L CO species using either 24% CO/He or 24% CO/H<sub>2</sub> whereas CH<sub>4</sub> is produced in the presence of hydrogen showing that the L CO adsorption equilibrium is not disturbed by the CH<sub>4</sub> production. In part 1 [1], it has been shown that these data are consistent with (a) calculations using the Temkin-C model and (b) the fact that the coverage of the L CO species for 1% CO/H<sub>2</sub> is only slightly lower than that using 1% CO/He for  $T > 580$  K. The studies of Vannice et al. [17,18,21] strongly suggest developing the EMA approach of the CO/H<sub>2</sub> reaction on the present Pt particles by considering that the L CO species is the adsorbed intermediate and by studying the impact of the CH<sub>4</sub> production on its coverage. This imposes the selection of plausible surface elementary steps involving the L CO species in the formation of CH<sub>4</sub>. Then, the rate  $R_s$  of consumption of the L CO species may or not disturb its competitive adsorption equilibrium with hydrogen species according to the reaction equilibrium.

### 3.4. Choice of the surface elementary steps implying the L CO species in the CO/H<sub>2</sub> reaction

Considering the CH<sub>4</sub> production from CO/H<sub>2</sub> gas mixtures on Pt particles, two plausible surface elementary steps can be proposed for the perturbation of the adsorption equilibrium of the L CO species either the direct or the hydrogen-assisted CO dissociation which are the topic of scientific debates on the mechanism of the CO hydrogenation on metal surfaces [22–32]. Experimental studies and DFT calculations on different metal surfaces such as Ru [24], Co [25–27], Ni [28] and Fe [29] lead to the conclusion that the

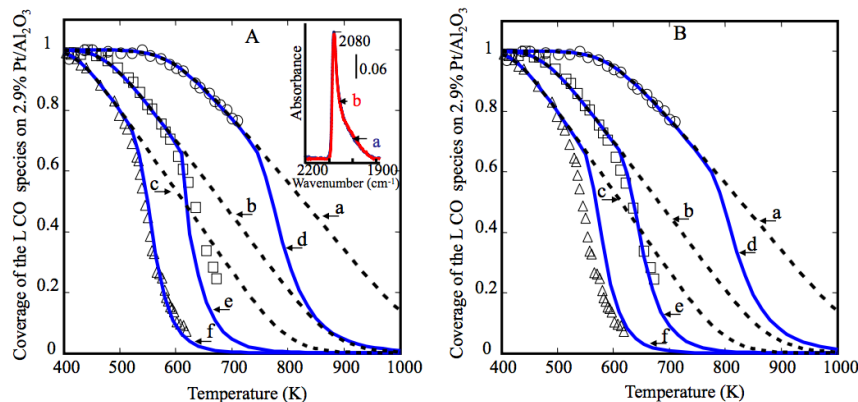


**Fig. 2.** Comparison of the experimental data during the adsorption/reaction of  $x\%$  CO/H<sub>2</sub> on 2.9% Pt/Al<sub>2</sub>O<sub>3</sub> ( $D = 0.26$ ) to theoretical curves obtained from the Temkin-C (competitive adsorption CO-H<sub>2</sub>) and Temkin-C.R (competitive adsorption CO-H<sub>2</sub> associated with the CH<sub>4</sub> production) models considering isobaric conditions. ○, □ and Δ experimental coverages of the L CO species for  $x\%$  CO/H<sub>2</sub> with  $x = 1, 10^{-2}$  and  $10^{-3}$  respectively with the increase in the temperature; (a), (b), and (c) theoretical evolutions of the coverage of the L CO species according to the Temkin-C model [1] with  $x = 1, 10^{-2}$  and  $10^{-3}$  respectively; (d), (e) and (f) theoretical evolutions of the coverage of the L CO species according to the Temkin-C.R model  $x = 1, 10^{-2}$  and  $10^{-3}$  respectively. **Parts A and B:** Temkin-C.R model using an activation energy for the hydrogenation surface elementary step (Eq. (4)) of 150 and 155 kJ/mol respectively (see the text for more details). **Inset Part A:** Comparison of the intensity of the IR band of the L CO species at 300 K using 1% CO/H<sub>2</sub> (a) and  $10^{-3}\%$  CO/H<sub>2</sub> (b).

**Table 1**

Heats of adsorption ( $E(\theta)$  with  $\theta$  the coverage) of L CO, 3FC CO and dissociated hydrogen species and activation energy of hydrogenation of the adsorbed CO species used for the comparison of the experimental data to the Temkin-C [1], Temkin-C.R., Langmuir-C.R and pseudo Langmuir-C.R models.

Adsorbed species	Heat of adsorption $E(\theta)$ (kJ/mol)	Activation energy $E_r$ (kJ/mol)
<i>Temkin-C model</i>		
L CO	$E(0) = 206^a$	$E(1) = 115^a$
H <sub>ads</sub>	$E(0) = 115^b$	$E(1) = 77^b$
<i>Temkin-C.R model</i>		
L CO	$E(0) = 206^a$	$E(1) = 115^a$
H <sub>ads</sub>	$E(0) = 115^b$	$E(1) = 77^b$
<i>Temkin-C.R model</i>		
3FC CO	$E(0) = 135^a$	$E(1) = 104^a$
H <sub>ads</sub>	$E(0) = 115^b$	$E(1) = 77^b$
<i>Langmuir-C.R model</i>		
L CO	$E = 138^c$	$E_r = 120^d$
H <sub>ads</sub>	$E = 90^c$	
<i>Pseudo-Langmuir-C.R model</i>		
L CO	$E(0) = 190^c$	$E(1) = 130^c$
H <sub>ads</sub>	$E(0) = 96^c$	$E(1) = 88^c$

<sup>a</sup> Ref. [5].

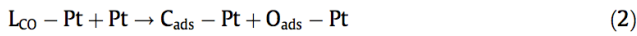
<sup>b</sup> Ref. [11].

<sup>c</sup> Ref. [1].

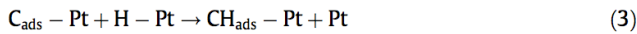
<sup>d</sup> The present study.

hydrogen assisted CO dissociation is more favorable than the direct dissociation. However, DFT calculations on Ru and Co may lead to the opposite conclusions [22,23]. On the present 2.9% Pt/Al<sub>2</sub>O<sub>3</sub>, the direct L CO dissociation can be envisaged as providing adsorbed surface carbon atom C<sub>ads</sub> leading to the CH<sub>4</sub> production via successive surface hydrogenation elementary steps providing CH<sub>xads</sub> species ( $x = 1$  to 4) according to:

Dissociation of the L CO species:



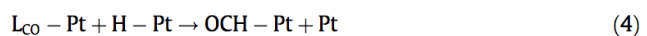
Hydrogenation of the elementary carbon C<sub>ads</sub>:



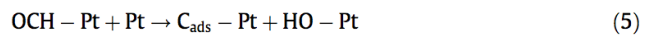
Note that elementary steps (2) and (3) impose free Pt sites for the L CO dissociation and hydrogen adsorption. These Pt sites can

be either those liberated at high temperatures after the decrease in the coverage of the L CO species due to its heat of adsorption at high coverage or to those liberated at low temperatures by the desorption of the B and/or 3FC CO species having heats of adsorption smaller than that of the L CO species [5]. Steps (2) and (3) have not been considered in the present EMA for the following argument. The CO dissociation (Eq. (2)) must exist in the absence of hydrogen. However, we have shown that successive heating (to 713 K) /cooling (to 300 K) cycles in 1% CO/He have no impact on the intensity of the IR band of the L CO species on 2.9% Pt/Al<sub>2</sub>O<sub>3</sub> [3–5]. This indicates that there is no accumulation of C<sub>ads</sub> species due to the CO dissociation. This is not the situation for the adsorption of 1% CO/He on a 10% Co/Al<sub>2</sub>O<sub>3</sub> catalyst: the CO dissociation leads at  $T > 440$  K to the modification of the Co<sup>o</sup> particles by the insertion of C<sub>ads</sub> species in the surface and then in the bulk whereas at  $T_a > 610$  K their accumulation on the surface decreases the amount of the Co sites [10]. This suggests that the activation of L CO species in the CH<sub>4</sub> production on 2.9% Pt/Al<sub>2</sub>O<sub>3</sub> imposes the presence of adsorbed hydrogen species via the hydrogen-assisted CO dissociation [22–29]. This is consistent with the DFT calculations of Neurock [33] on the CO/H<sub>2</sub> reaction on Pd<sub>x</sub> particles with  $x$  in the 1–19 range. The author shows that (a) the activation of adsorbed CO on Pd(111) by direct dissociation of CO is highly endothermic (+200 kJ/mol) and (b) the reaction of adsorbed CO and hydrogen species (via a migratory insertion of the CO into a Pd–H bond) to form formyl (CHO<sub>ads</sub>) is favorable (in the range (+70) – (+80) kJ/mol according to the Pd cluster size (Pd<sub>1</sub>, Pd<sub>2</sub>, Pd<sub>19</sub>)). Moreover, Neurock [33] shows that the successive hydrogenation surface elementary steps from the formyl to CH<sub>4</sub> are all exothermic indicating that the limiting step is the first hydrogenation of the adsorbed CO species. The hydrogen assisted L CO dissociation on the present 2.9% Pt/Al<sub>2</sub>O<sub>3</sub> catalyst can be represented by the following surface elementary steps:

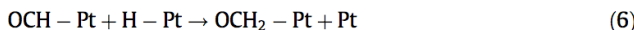
Activation of the L CO species by adsorbed hydrogen species forming formyl species:



Followed by either the decomposition of the formyl species leading to carbon atom:



or the insertion of a second hydrogen species:



Then successive hydrogenation surface elementary steps from C<sub>ads</sub> in step (5) or from H<sub>2</sub>CO in step (6) via adsorbed methoxyl species lead to the CH<sub>4</sub> production. Similar surface elementary steps can be proposed assuming that the activation of the L CO species by adsorbed hydrogen species leads to the formation of adsorbed carbon-hydroxyl COH. Note that Vannice [34] suggests that the activation of the intermediate adsorbed CO species by hydrogen on Pt proceeds according to the following surface elementary steps:



However, the adsorption of hydrogen on 2.9% Pt/Al<sub>2</sub>O<sub>3</sub> is mainly dissociative [1] and the surface elementary steps (4)-(6) seems more consistent with the experimental data.

The rate of consumption of the L CO species according to Eq. (4) corresponds to that of a Langmuir-Hinshelwood surface elementary step:

$$R_r = k_r \theta_{\text{LCO}} \theta_H \quad (8)$$

with k<sub>r</sub> the rate constant, θ<sub>LCO</sub> and θ<sub>H</sub> the coverage of the L CO and dissociated hydrogen species provided by the Temkin-C.R model. Note that whatever the activation energy of step (4), its rate can be significant only at high temperatures after the decrease (according to the experimental conditions: P<sub>CO</sub>, p<sub>H2</sub> and T) in the coverage of the L CO species to allow the adsorption of hydrogen. Moreover, if the rate of step (4) is faster than those of steps (5) or (6) then the IR band of the L CO species must decrease whereas that of the new adsorbed species (i.e. OCH-Pt) must increase until a steady state. However, (a) the L CO species is observed until 715 K in 1% CO/H<sub>2</sub> (Fig. 1) whereas the rate of CH<sub>4</sub> production is significant and (b) the IR bands of adsorbed CH<sub>x</sub>O species formed in parallel to the CH<sub>4</sub> production, on the 2.9% Pt/Al<sub>2</sub>O<sub>3</sub> catalyst during the CO/H<sub>2</sub> reaction, have been ascribed in agreement with literature data to formate species on the alumina support [1]. Their accumulation on the catalyst is due to their very low reactivity with hydrogen and/or a low rate of decomposition allowing their detection at 713 K in the presence of 1% CO/H<sub>2</sub> [1]. This suggests, in agreement with the conclusion of Neurock [33] on Pd<sub>x</sub> clusters that the rate of the elementary step (4) is lower than the successive hydrogenation elementary steps leading to CH<sub>4</sub>. This prevents the accumulation of a significant amount of intermediate species between L CO species and CH<sub>4</sub>. Finally, the Temkin-C.R model has been developed by considering that the L CO and dissociated hydrogen species adsorbed on the same Pt sites (competitive chemisorption) of 2.9% Pt/Al<sub>2</sub>O<sub>3</sub>, react at high temperatures according to the surface elementary step (4) which is the limiting step of the CH<sub>4</sub> production.

### 3.5. Temkin-C.R model for the CO/H<sub>2</sub> reaction on 2.9% Pt/Al<sub>2</sub>O<sub>3</sub>

Similarly to Part 1 [1], the Temkin-C.R model is developed using the integral equation approach (abbreviation IE) [35–37]. It is considered that the Pt sites in a number N are constituted of i groups (i = 0 to m) with N<sub>i</sub> sites having the same adsorption/catalytic properties such as N = ∑<sub>i=0</sub><sup>m</sup> N<sub>i</sub>. On each group, the local coverages of CO and hydrogen (denoted A and B respectively to simply the presentation of the Temkin-C.R model) are provided by two reaction equilibria according to the Langmuir formalism: R<sub>a</sub> - R<sub>d</sub> - R<sub>s</sub> = 0 where (a) R<sub>a</sub> and R<sub>d</sub>, are the rates of adsorption and desorption of either CO or H<sub>2</sub> forming the L CO and dissociated hydrogen species respectively and (b) R<sub>s</sub> is the rate of the surface reaction (Eq. (4)). The Langmuir formalism leads to the following set of equations:

– For the L CO species

$$kA_a P_A (1 - \theta_A - \theta_B) - kA_d \theta_A - k_r \theta_A \theta_B = 0 \quad (9)$$

– For the dissociated hydrogen species

$$2kB_a P_B (1 - \theta_A - \theta_B)^2 - 2kB_d \theta_B^2 - k_r \theta_A \theta_B = 0 \quad (10)$$

where kA<sub>a</sub> (kB<sub>a</sub>) and kA<sub>d</sub> (kB<sub>d</sub>) are the rate constants of adsorption and desorption of A (B) respectively (in Eq. (10) the factor 2 comes from the stoichiometry of the dissociative H<sub>2</sub> chemisorption) and k<sub>r</sub> is the rate constant of the surface elementary step (4). By dividing Eqs. (9) and (10) by kA<sub>d</sub> and kB<sub>d</sub> respectively a new set of equations are obtained related to the adsorption coefficients (KA<sub>a</sub> = kA<sub>a</sub>/kA<sub>d</sub> and KB<sub>a</sub> = kB<sub>a</sub>/kB<sub>d</sub>) and the reaction coefficients (KA<sub>r</sub> = k<sub>r</sub>/kA<sub>d</sub> and KB<sub>r</sub> = k<sub>r</sub>/kB<sub>d</sub>):

– For the L CO species, Eq. (9) leads to:

$$KA_a P_A (1 - \theta_A - \theta_B) - \theta_A - KA_r \theta_A \theta_B = 0 \quad (11)$$

– For the dissociated hydrogen species, Eq. (10) leads to:

$$2KB_a P_B (1 - \theta_A - \theta_B)^2 - 2\theta_B^2 - KB_r \theta_A \theta_B = 0 \quad (12)$$

Similarly to previous works, for the adsorbed species formed by A and B, the adsorption coefficients are provided by the statistical thermodynamics assuming localized adsorbed species [1,3–11]:

$$\begin{aligned} KX_a(\text{EX}) &= \frac{h^3}{(2\pi m_X)^{3/2}} \frac{1}{(kT)^{5/2}} \exp\left(\frac{\text{EX}_d - \text{EX}_a}{RT}\right) \\ &= A(T) \exp\left(\frac{\text{EX}}{RT}\right) \end{aligned} \quad (13)$$

where h and k are Planck's and Boltzmann's constants, R is the ideal gas constant, X is either A or B, m<sub>X</sub> is the mass of the molecule, T is the temperature and EX<sub>d</sub> and EX<sub>a</sub> are the activation energies of desorption and adsorption respectively. For non activated chemisorption such as CO and H<sub>2</sub> on Pt particles, EX<sub>a</sub> = 0 and EX = EX<sub>d</sub> is the heat of adsorption. For the heterogeneous surface of the Pt particles EX (and so KX<sub>a</sub>) is dependent on the coverage of the surface by the adsorbed species formed by X.

The expression of the reaction coefficient according to the transition state theory can be obtained from (a) the expressions of the rate constant of desorption for A and B:

$$kA_d = \left(\frac{kT}{h}\right) \exp\left(-\frac{EA_d}{RT}\right) \quad \text{and} \quad kB_d = \left(\frac{kT}{h}\right) \exp\left(-\frac{EB_d}{RT}\right) \quad (14)$$

and (b) the rate constant of a Langmuir- Hinshelwood elementary step such as Eq. (4):

$$k_r = \left(\frac{kT}{h}\right) \exp\left(-\frac{E_r}{RT}\right) \quad (15)$$

where E<sub>r</sub> is the activation energy of step (4). For non activated chemisorption the expressions of the reaction coefficients for A and B are:

$$\begin{aligned} KA_r(EA - E_r) &= \exp\left(\frac{EA - E_r}{RT}\right) \quad \text{and} \quad KA_r(EB - E_r) \\ &= \exp\left(\frac{EB - E_r}{RT}\right) \end{aligned} \quad (16)$$

According to the IE approach [35–37] Eqs. (11) and (12) can be applied at each group i having N<sub>i</sub> sites characterized by heats of adsorption EA<sub>i</sub> and EB<sub>i</sub> whereas we assume in the first stage of development of the Temkin-C.R model that E<sub>r</sub> is the same for each group of sites (this means that the heterogeneity of the surface concerns mainly the heats of adsorption of A and B). This leads to a set of equations giving the local coverage θA<sub>i</sub> and θB<sub>i</sub> of A and B species on the group i having N<sub>i</sub> sites:

For the adsorbed species A:

$$KA_a(EA_i) \quad P_A \quad (1 - \theta_{Ai} - \theta_{Bi}) - \theta_{Ai} - KA_{ri}(EA_i - E_r) \quad \theta_{Ai} \quad \theta_{Bi} = 0 \quad (17)$$

For the adsorbed species B:

$$2KB_a(EB_i) \quad P_B \quad (1 - \theta_{Ai} - \theta_{Bi})^2 - 2\theta_{Bi}^2 - KB_{ri}(EB_i - E_r) \quad \theta_{Ai} \quad \theta_{Bi} = 0 \quad (18)$$

Assuming that the m groups of sites have heats of adsorption varying linearly between EA<sub>0</sub> and EA<sub>1</sub> and EB<sub>0</sub> and EB<sub>1</sub> for A and B respectively (Temkin formalism see Refs. [3–5,11] and Part 1 [1]) then the heats of adsorption of A and B on each group of sites are:

$$EA_i = EA_0 + \frac{i}{m}(EA_1 - EA_0) \text{ with } EA_0 \text{ and } EA_1 \\ \text{for } i = 0 \text{ and } m \text{ respectively} \quad (19)$$

$$EB_i = EB_0 + \frac{i}{m}(EB_1 - EB_0) \text{ with } EB_0 \text{ and } EB_1 \\ \text{for } i = 0 \text{ and } m \text{ respectively} \quad (20)$$

For a temperature T<sub>j</sub> in the 300–900 K range, the numerical resolution of Eqs. (17) and (18) (using the *raider* function of Mathcad) gives the local coverages θA<sub>i</sub>(T<sub>j</sub>) and θB<sub>i</sub>(T<sub>j</sub>) for A and B on the group i having N<sub>i</sub> sites (heats of adsorption provided by (19)–(20)) for fixed values of P<sub>A</sub>, P<sub>B</sub> and T<sub>j</sub>. These calculations can be repeated for the same T<sub>j</sub>, P<sub>A</sub> and P<sub>B</sub> values to obtain the local coverage of A and B on each of the m groups of sites. Then, for the group i having N<sub>i</sub> sites the amounts of adsorbed species formed by A and B at T<sub>j</sub> are:

$$nA_i(T_j) = \theta A_i(T_j) N_i \quad \text{and} \quad nB_i(T_j) = \theta B_i(T_j) N_i \quad (21)$$

and the total amounts nA and nB of A and B on the surface (on the m groups of sites) at T<sub>j</sub> are:

$$nA = \sum_{i=0}^m nA_i(T_j) = \sum_{i=0}^m \theta A_i(T_j) N_i \quad \text{and} \quad nB = \sum_{i=0}^m nB_i(T_j) \\ = \sum_{i=0}^m \theta B_i(T_j) N_i \quad (22)$$

which give the coverage of the N sites of the Pt surface by A and B at T<sub>j</sub> for P<sub>A</sub> and P<sub>B</sub>:

$$\theta A(T_j) = \frac{nA}{N} = \sum_{i=0}^m \theta A_i(T_j) \frac{N_i}{N} \quad \text{and} \quad \theta B(T_j) = \frac{nB}{N} \\ = \sum_{i=0}^m \theta B_i(T_j) \frac{N_i}{N} \quad (23)$$

In line with the IE approach [35–37] of the Temkin-C model [1], assuming a continuous distribution of the sites then N<sub>i</sub> = dN with dN/N from the Temkin formalism [1]:

$$\frac{dN}{N} = \frac{dE_A}{\Delta E_A} = \frac{dE_B}{\Delta E_B} \text{ with } \Delta E_A = EA_0 - EA_1 \text{ and } \Delta E_B \\ = EB_0 - EB_1 \quad (24)$$

Note that as discussed in Part 1 [1], Eq. (24) signifies that the heats of adsorption of A and B linearly vary with either coverages whatever the origin (intrinsic and/or induced) of the heterogeneity. Using Eq. (24), the sums in (23) can be transformed into an integral by modeling via interpolation (using the *cspline* and *interpret* function of Mathcad) the two set of data (θA<sub>i</sub>(T<sub>j</sub>), EA<sub>i</sub>) and (θB<sub>i</sub>(T<sub>j</sub>), EB<sub>i</sub>). Denoting f(EA) and g(EB) the interpolated curves then:

$$\theta A(T_j) = \int_{EA_0}^{EA_1} f(E_A) \frac{dE_A}{\Delta E_A} \quad (25)$$

$$\theta B(T_j) = \int_{EB_0}^{EB_1} g(E_B) \frac{dE_B}{\Delta E_B} \quad (26)$$

Eqs. (25) and (26) give for the temperature T<sub>j</sub> and adsorption pressures P<sub>A</sub> and P<sub>B</sub>, the coverage of the A and B adsorbed species according to the Temkin-C.R model. These calculations can be performed for the different T<sub>j</sub> values. In the present study the calculations have been performed by step of 1 K in the range 300–1000 K, providing the theoretical evolutions of the coverages of the A and B adsorbed species according to the Temkin-C.R model during the increase in T. Note that P<sub>A</sub> and P<sub>B</sub> are considered constant (isobaric conditions) in the different calculations even during the CH<sub>4</sub> production from the hydrogenation of the L CO species. This is reasonable for hydrogen which is present in large excess in the present x% CO/H<sub>2</sub> gas mixtures. For CO, this assumption can be considered valid for CO conversions lower than ≈ 20% because it has been shown in Part 1 [1] that a factor of two on P<sub>A</sub> has a limited impact on the coverage of the adsorbed species (the difference is in the range of the experimental uncertainties). The calculations have been performed assuming in Eqs. (19) and (20) that the number of groups sites is m = 30, however this value can be selected in a large range (except small values: m < ≈ 5) without significant modifications of the profile of the evolution of the coverages of the L CO and hydrogen species due the mathematical procedure selected in Eqs. (25) and (26).

### 3.6. Coverages of L CO and hydrogen species from the Temkin-C.R. Model for x% CO/H<sub>2</sub>

Curves d, e and f in Fig. 2A give, for x = 1, 10<sup>-2</sup> and 10<sup>-3</sup> respectively, the theoretical evolutions of the coverage of the L CO species on 2.9% Pt/Al<sub>2</sub>O<sub>3</sub> according to the Temkin-C.R model using Eqs. (25) and (26) with the parameters of Table 1. The heats of adsorption of the L CO and hydrogen adsorbed species in the calculations are the same that those used for the Temkin-C model [1] whereas the activation energy of the surface elementary step (4) is E<sub>r</sub> = 150 kJ/mol.

The E<sub>r</sub> value provides theoretical curves consistent with the experimental data in the full range of temperature for P<sub>CO</sub> = 1 kPa and 1 Pa in the CO/H<sub>2</sub> gas mixtures (curves d and f in Fig. 2A respectively) whereas the theoretical coverage is slightly lower than the experimental data for P<sub>CO</sub> = 10 Pa. This is due to the high sensitivity of the Temkin-C.R model to the E<sub>r</sub> value. For instance, Fig. 2B compares the experimental and theoretical coverage considering E<sub>r</sub> = 155 kJ/mol. This leads to theoretical curves consistent with the experimental data for P<sub>CO</sub> = 1000 Pa and 10 Pa (curves d and e in Fig. 2B respectively) whereas for P<sub>CO</sub> = 1 Pa the theoretical curve f is higher than the experimental data at high temperatures. This can be explained considering that the decrease in the CO pressure due to the CH<sub>4</sub> production is more significant for P<sub>CO</sub> = 1 Pa than for higher CO partial pressures leading to lower experimental coverage than those of the Temkin-C.R model which assumes isobaric conditions. Finally, it can be considered that E<sub>r</sub> is slightly dependent on the coverage of the L CO species and so of the partial pressure of CO: three theoretical curves, consistent with the experimental data are obtained using E<sub>r</sub> = 160, 155 and 150 kJ/mol for P<sub>CO</sub> = 1000, 10 and 1 Pa respectively (result not shown). It must be noted that for 1% CO/H<sub>2</sub> the theoretical coverage of the L CO species remains equal to ≈ 1 until ≈ 500 K which is the temperature determined by Panagiotopoulou et al. [20] for the CH<sub>4</sub> production from 1% CO/50% H<sub>2</sub>/He on 0.5% Pt/Al<sub>2</sub>O<sub>3</sub>.

Fig. 3 compares the theoretical coverages of the L CO and hydrogen adsorbed species on 2.9% Pt/Al<sub>2</sub>O<sub>3</sub> from the three following models: Temkin, Temkin-C and Temkin-C.R using the heats of adsorptions in Table 1 with an activation energy for step (4) of 150 kJ/mol. Curves a and b correspond to the coverages of the L CO and hydrogen species respectively in the absence of competition (Temkin adsorption model) [3–5,11] for P<sub>CO</sub> = 1 kPa and

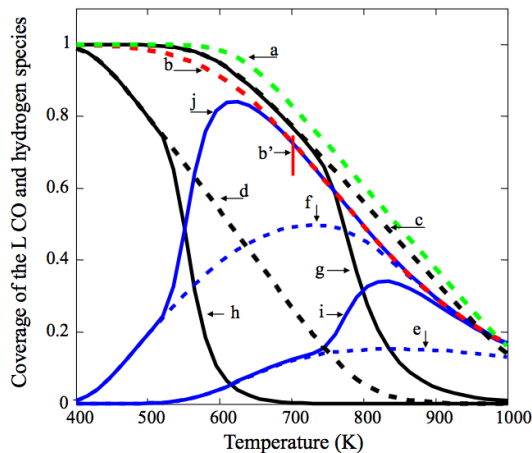


**Fig. 3.** Theoretical coverages of the L CO and hydrogen species on the reduced 2.9% Pt/Al<sub>2</sub>O<sub>3</sub> catalyst for the different models based on the Temkin formalism according to the experimental conditions: (a) and (b) coverage of the L CO and hydrogen species in the absence of competition using 1% CO/He and pure hydrogen according to the Temkin adsorption model (from Refs. [3–5,11]); b': estimation of the coverage of the hydrogen species at 713 K for p<sub>H2</sub> = 10<sup>5</sup> Pa using FTIR spectroscopy; (c) and (d) ((e) and (f)) coverage of the L CO species (hydrogen species) in competitive adsorption with hydrogen according to the Temkin-C model for 1% CO/H<sub>2</sub> and 10<sup>-3</sup>% CO/H<sub>2</sub> respectively; (g) and (h) ((i) and (j)) coverage of the L CO species (hydrogen species) during the CO/H<sub>2</sub> reaction according to the Temkin-C.R model for 1%CO/H<sub>2</sub> and 10<sup>-3</sup>% CO/H<sub>2</sub> respectively (see the text for more details).

p<sub>H2</sub> = 10<sup>5</sup> Pa. Curves c (e) and d (f) correspond to the coverages of the L CO (hydrogen) species according to the Temkin-C model for 1% CO/H<sub>2</sub> and 10<sup>-3</sup>% CO/H<sub>2</sub> respectively. For P<sub>CO</sub> = 1 kPa, the comparison of curves a and c shows that the competitive CO-H<sub>2</sub> chemisorption decreases slightly the coverages of the L CO species for T > 500 K. For p<sub>H2</sub> = 10<sup>5</sup> Pa, the comparison of curves b and e shows that the coverage of the hydrogen species is strongly decreased particularly at low temperatures in the presence of CO (from 1 to 0 for T < 500 K). Curves b and f show that the coverage of the hydrogen species is also significantly decreased for P<sub>CO</sub> = 1 Pa.

Curves g (i) and h (j) in Fig. 3 give the coverages of the L CO (hydrogen) species according to the Temkin-C.R model for 1% CO/H<sub>2</sub> and 10<sup>-3</sup>% CO/H<sub>2</sub> respectively. For 1% CO/H<sub>2</sub>, the comparison of curves c and e from the Temkin-C model with curves g and i respectively from the Temkin-C.R shows how the rate of the surface elementary step (4) disturbs the competitive adsorption equilibriums of the L CO and hydrogen species: at T > 730 K the coverage of L CO species decreases associated with the increase in the coverage of the hydrogen species, until values equal to the coverage of the hydrogen species in the absence of CO at T > 940 K (curve b). Similar conclusions are obtained for 10<sup>-3</sup>% CO/H<sub>2</sub> except that the comparison of curves f and j shows that the impact of step (4) is stronger for T > 520 K.

The validity of the present Temkin-C.R model is justified by the fact that the theoretical coverages of the L CO species for the three partial pressures of CO are consistent with the experimental data (Fig. 2). For the coverage of the hydrogen species they are different difficulties which prevent obtaining similar experimental data. However semi quantitative data on the coverage of the hydrogen species using 10<sup>-3</sup>% CO/H<sub>2</sub> have been obtained confirming the validity of the present Temlin-C.R model for this reactant.

### 3.7. Experimental coverage of the hydrogen species during the CO/H<sub>2</sub> reaction

In the absence of CO, the evolution of the coverage of the hydrogen species during the increase in the adsorption temperature in

the 300–713 K range has been obtained via the net rate of desorption of hydrogen (based on hydrogen mass balance with the M.S system) in the presence (TPAE procedure) or not (TPD with read-sorption) of a small partial pressure of hydrogen in the inlet gas flow rate (i.e. 0.5% H<sub>2</sub>/0.5% Ar/He) [11]. The very low intensity of the IR band of hydrogen species adsorbed on 2.9% Pt/Al<sub>2</sub>O<sub>3</sub> prevented using the AEIR method. However, the quantification of the hydrogen coverage using the M.S system cannot be applied for the CO/H<sub>2</sub> reaction (even for a semi-quantitative approach) because (a) the amounts of adsorbed hydrogen is very low in the temperature range 300–550 K and (b) for T > 550 K, the CH<sub>4</sub> formation leads to a significant hydrogen consumption which dominates the others surface processes preventing accurate values of the hydrogen coverage from hydrogen mass balance. In the presence of CO, FTIR spectroscopy is more appropriate to obtain semi quantitative experimental data on the change in the coverage of the hydrogen species. For instance, spectra a and b in Fig. 4 have been recorded before and after the adsorption of p<sub>H2</sub> = 10<sup>5</sup> Pa at 300 K respectively on the reduced 2.9% Pt/Al<sub>2</sub>O<sub>3</sub> solid. The adsorption of hydrogen, leads to a very small IR band at 2115 cm<sup>-1</sup>: its intensity is lower, by a factor ≈80, than the IR band of the L CO after saturation of the Pt sites at 300 K using 10<sup>-3</sup>% CO/H<sub>2</sub> (Fig. 4, spectrum c).

Literature data on FTIR studies of the adsorption of hydrogen on 10% Pt/Al<sub>2</sub>O<sub>3</sub> [38,39], indicate the presence of an IR band at 2120 cm<sup>-1</sup> ascribed to v(Pt-H) due to the dissociative adsorption of hydrogen on the Pt particles. This IR band can be associated with an IR band at 2060 cm<sup>-1</sup> (often detected as a shoulder of the IR band at 2120 cm<sup>-1</sup>) ascribed to a second type of Pt-H bond [39,40]. The intensity ratio between the two IR bands is dependent on different parameters such as the Pt particle size, the reduction temperature and the nature of the support [38–40]. The detection by using IR spectroscopy of Pt-H species is often mentioned in literature data dedicated to the electrochemical hydrogen formation from Pt electrodes in the presence of acidic aqueous solutions [41–44]. As discussed by different authors [38–40] using D<sub>2</sub> adsorption [38,39], an IR band below 2100 cm<sup>-1</sup> after hydrogen adsorption on Pt particles can be due to a linear CO species on the Pt sites formed by the adsorption of CO impurities. According to Refs. [39,40], the IR band at 2115 cm<sup>-1</sup> in spectrum b of Fig. 4 is ascribed to Pt-H bonds due to the dissociative adsorption of H<sub>2</sub>. Spectrum d in

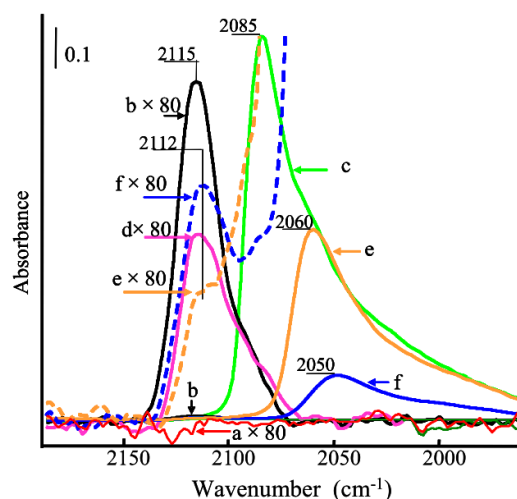


**Fig. 4.** IR spectra of the adsorbed hydrogen and L CO species on the reduced 2.9% Pt/Al<sub>2</sub>O<sub>3</sub> catalyst for different experimental conditions. (a) IR spectrum of the solid at 300 K (background) before hydrogen adsorption; (b) adsorption of 10<sup>5</sup> Pa of hydrogen at 300 K; (c) adsorption of 10<sup>-3</sup>% CO/H<sub>2</sub> at 300 K; (d) adsorption of 10<sup>5</sup> Pa of hydrogen at 713 K; (e) and (f) adsorption/reaction of 10<sup>-3</sup>% CO/H<sub>2</sub> at 573 K and 615 K respectively.

**Fig. 4** gives the intensity of this IR band for the adsorption of  $P_{H_2} = 10^5$  Pa at  $T_a = 713$  K on 2.9% Pt/Al<sub>2</sub>O<sub>3</sub>. Considering the saturation of the Pt sites after adsorption of hydrogen at 300 K [11] then the coverage of the sites at 713 K can be estimated (Eq. (1)) in the range 0.72–0.59 due to the difficulties in the accurate determination of the area of the IR band at 2115 cm<sup>-1</sup> in spectra b and d of **Fig. 4**. This estimation of the hydrogen coverage is reported as a bar graph (denoted b') in **Fig. 3** showing that it is consistent with the coverage of the hydrogen (curve b) in the absence of CO [11]. In the temperature range 300–550 K, the IR band of the Pt-H species is not detected in the presence of 10<sup>-3</sup>% CO/H<sub>2</sub>: this is consistent with the competitive chemisorption in favor of the L CO species (**Fig. 3** curve f). However at 573 K, after the significant decrease in the coverage of the L CO species (see **Fig. 2** and compare spectra c and e in **Fig. 4**) due to step (4), a shoulder is detected at 2112 cm<sup>-1</sup> (spectrum e in **Fig. 4**) which increases with  $T$  (spectrum f in **Fig. 4**) associated with the strong decrease in the coverage of the L CO species. The increase in the amount of the adsorbed hydrogen species with the increase in  $T$  in parallel with the decrease in the L CO coverage is consistent with the theoretical curves from the Temkin-C.R model (**Fig. 3**, curves j and h respectively) and confirms the strong impact of step (4) on the two coverages.

**Figs. 2 and 3** show that the Temkin-C.R model provides a reasonable interpretation of the evolution of the coverages of (a) the L CO species for the three  $x\%$  CO/H<sub>2</sub> gas mixtures and (b) the adsorbed hydrogen species for 10<sup>-3</sup>% CO/H<sub>2</sub>. This permits the evaluation of the theoretical rate of CH<sub>4</sub> production from the reaction between the L CO and hydrogen adsorbed species on the same Pt sites which can be compared to the experimental rate. This comparison must be performed at low CO conversions because the present Temkin-C.R model assumes isobaric conditions for CO and hydrogen whatever  $T$ .

### 3.8. Temkin-C.R model and rate of the CH<sub>4</sub> production

Using the M.S system, curve a in **Fig. 5** gives the experimental evolution of the rate of the CH<sub>4</sub> production on the reduced 2.9% Pt/Al<sub>2</sub>O<sub>3</sub> catalyst during the increase in the reaction temperature for 1% CO/H<sub>2</sub>. The experimental rate of CH<sub>4</sub> production is expressed in TOF as:

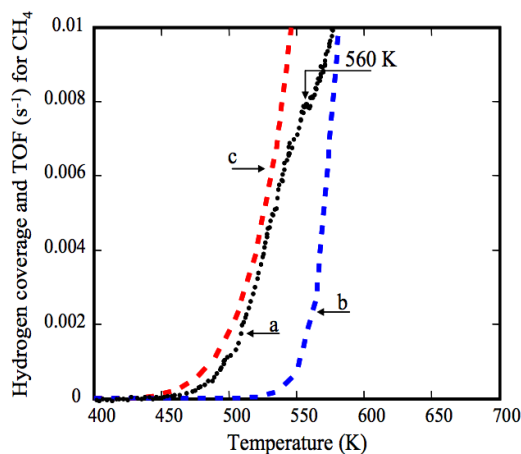


**Fig. 5.** Comparison of the experimental rate of the CH<sub>4</sub> formation at low CO conversions (<10%) for 1% CO/H<sub>2</sub> on 2.9% Pt/Al<sub>2</sub>O<sub>3</sub> to the theoretical rate from the Temkin-C.R model considering a reaction between L CO and hydrogen adsorbed species. (a) experimental rate of the CH<sub>4</sub> production; (b) theoretical rate and (c) theoretical hydrogen coverage from the Temkin-C.R model considering an activation energy  $E_r = 150$  kJ/mol for the hydrogenation of the L CO species (step (4)).

$$TOF_{CH_4}(s^{-1}) = \frac{R_{CH_4}}{Q_{Pt}} \quad (27)$$

with  $R_{CH_4}$  the experimental rate (in  $\mu\text{mol of CH}_4 \text{ g}^{-1} \text{ s}^{-1}$ ) and  $Q_{Pt}$  (in  $\mu\text{mol Pt g}^{-1}$ ) the amount of Pt adsorption sites involved in the activation of CO and quantified by the amount of CO adsorbed at 300 K at saturation of the Pt surface (mainly the L CO species): 48  $\mu\text{mol/g}$  [1]. The rate is measured for CO conversions lower than 10% (a) to prevent mass transfer limitations [1] (in particular by the evaluation: 0.15 of the Weisz-Prater criterion [45] at  $T = 600$  K) and (b) to consider that the decrease in the CO partial pressure due to the CH<sub>4</sub> production has no significant impact on the calculations based on isobaric condition [1]. The comparison of the FTIR data: **Fig. 1** and experimental coverage of the L CO species in **Fig. 2**, to similar data obtained in a previous study dedicated to the EMA of the CO/O<sub>2</sub> reaction on the present 2.9% Pt/Al<sub>2</sub>O<sub>3</sub> catalyst [46], justifies the absence of a significant contribution of mass transfer limitations during the FTIR measurements. It has been shown that the evolution of the IR band of the L CO species, in parallel to the CO<sub>2</sub> production, during the increase in the temperature for 1% CO/y% O<sub>2</sub>/He in excess O<sub>2</sub> strongly decreases (for CO conversions >~50%) at a temperature  $T_i$  dependent on  $y$  (i.e. for  $y = 1$  the coverage of the L CO species decreases for  $\approx 1$  at  $T_i = 507$  K to  $\approx 0.1$  at 511 K) associated with an overshoot in the CO<sub>2</sub> production.

These data are ascribed according to literature data [46] and references therein, to the strong perturbation of the reaction equilibrium of the L CO species by mass transfer limitations. The overshoot in the CO<sub>2</sub> production at  $T_i$  is ascribed to the fact that the excess of O<sub>2</sub> converts (a) CO in the gas phase and (b) a large fraction of the adsorbed CO species due to the limitation of the rate of CO transfer to the Pt sites. Similar observations (due to a strong mass transfer limitation) are not observed for the present study: (a) in **Fig. 2**, the coverage of the L CO species (in large excess of hydrogen) decreases progressively for the three  $x\%$  CO/H<sub>2</sub> gas mixtures with a profile consistent with a chemical reaction equilibrium involving the surface elementary step (4) according to the Temkin.C.R model and (b) there is no overshoot at high CO conversion in the CH<sub>4</sub> production during the increase in  $T$  [1].

For 1% CO/H<sub>2</sub>, **Fig. 5** shows that the CH<sub>4</sub> production (curve a) (a) starts at  $T \approx 475$  K which is a temperature consistent with literature data for different Pt containing solids and similar CO/H<sub>2</sub> gas mixtures [17–20] and (b) increases progressively with the increase in the reaction temperature (at 523 K the TOF is 0.003 s<sup>-1</sup> which is consistent with 0.002 s<sup>-1</sup> measured at this temperature by Panagiotopoulou et al. [20] on a 0.5 wt% Pt/Al<sub>2</sub>O<sub>3</sub> catalyst ( $D = 1$ ) using 1% CO/50% H<sub>2</sub>/He. There is an inflection point at  $\approx 560$  K in curve a of **Fig. 5** which is discussed in the following section. Assuming that step (4) is the rate limiting step of the CH<sub>4</sub> production then the experimental rate (curve a in **Fig. 5**) can be compared to the theoretical TOF ( $R_{CH_4}^{Theo.}$ ) from the Temkin-C.R model:

$$R_{CH_4}^{Theo.} = \frac{k}{h} \exp\left(\frac{-E_r}{RT}\right) \theta_{CO-L}^{theo} \theta_H^{theo} \quad (28)$$

where  $\theta_{CO-L}^{theo}$  and  $\theta_H^{theo}$  are the coverage of the L CO species and hydrogen species (curves g and i in **Fig. 3**) according to the Temkin.C.R model. Curves b and c in **Fig. 5** gives the evolution of  $R_{CH_4}^{Theo.}$  and the coverage of the hydrogen species respectively with the reaction temperature for 1% CO/H<sub>2</sub> considering the values of the heats of adsorption and activation energy of step (4) (**Table 1**) which provide  $\theta_{CO-L}^{theo}$  curves consistent with the experimental data (**Fig. 2A**). **Fig. 5** shows that curve b is significant different than the experimental data (curve a) at low temperatures: the CH<sub>4</sub> production starts at 475 K and 520 K for  $R_{CH_4}^{Exp.}$  and  $R_{CH_4}^{Theo.}$  respectively. An activation energy of  $E_r = 128$  kJ/mol must be used to obtain an agreement between experimental and theoretical rate of the reaction. However, this

value leads to a theoretical curve  $\theta_{CO-L}^{theo}$  from the Temkin-C.R model significant different than the experimental data for  $T > 600$  K (see Fig. S1 of Supporting Information). Considering the present EMA of the CO/H<sub>2</sub> reaction on 2.9% Pt/Al<sub>2</sub>O<sub>3</sub> based on the role of the L CO adsorbed species (which dominates the CO adsorption), this signifies that according to the Temkin-C.R model and considering that the activation energy of step (4) is independent on the coverage of surface: (a) the L CO cannot be considered as the active adsorbed species at the beginning ( $T \approx 475$  K for 1% CO/H<sub>2</sub>) of the CH<sub>4</sub> production (it may contribute to the CH<sub>4</sub> production for  $T \geq 520$  K) and (b) another CO hydrogenation route exists at the low temperature via an adsorbed CO species having activation energy of hydrogenation lower than the L CO species.

### 3.9. Temkin-C.R. Model and existence of two routes for the CH<sub>4</sub> production on Pt/Al<sub>2</sub>O<sub>3</sub>

The presence of two routes for the formation of CH<sub>4</sub> from the CO/H<sub>2</sub> reaction on Pt/Al<sub>2</sub>O<sub>3</sub> is consistent with literature data. For instance, Robbins and Marucchi-Soos [47] have studied by H<sub>2</sub>-TPR procedures the reactivity of the carbonaceous adsorbed species formed during the CO hydrogenation on 12 wt% Pt/Al<sub>2</sub>O<sub>3</sub> at  $T > 380$  K. Two overlapped CH<sub>4</sub> peaks are observed with maximum at  $T = 493$  K and  $T = 613$  K ascribed to the hydrogenation of the adsorbed methoxyl species (CH<sub>3</sub>O<sub>ads</sub>) and L CO adsorbed species respectively [47]. This indicates that the L CO species is not the adsorbed species having the highest reactivity for hydrogen [47]. The authors consider that the CH<sub>3</sub>O<sub>ads</sub> species are formed on Al<sup>+δ</sup> sites of the alumina support at the boundary of the Pt particles via hydrogenation of adsorbed CO species [47]. The Al<sup>+δ</sup> sites are formed by deshydroxylation of the support during the reduction procedure of the Pt particles at  $T > 573$  K. This is confirmed by the disappearance of the first CH<sub>4</sub> peak during H<sub>2</sub>-TPR (without modification of the second peak due to the L CO species) by rehydroxylation of the catalyst at 300 K after the reduction at 723 K [47]. The formation of adsorbed methoxyl species more reactive than adsorbed CO species during the CO/H<sub>2</sub> reaction have been confirmed by (a) the Falconer's group for the CO/H<sub>2</sub> reaction on Pd particles supported on different metal oxides [48–50] and (b) Vannice [51] who summarized literature data considering the involvement of the methoxyl species in the CH<sub>4</sub> formation from CO hydrogenation on different metal supported particles. The role of adsorbed methoxyl species on Pt and Pd has been confirmed by Shustorovich and Bell [52] using bond-order-conservation method. The authors conclude that (a) the assisted hydrogen dissociation of CO is favored leading to methoxyl species, (b) the cleavage of the bond between C and O occurs in the methoxyl species and (c) the dissociation/hydrogenation of CH<sub>3</sub>O<sub>ads</sub> to form CH<sub>4</sub> or CH<sub>3</sub>OH have similar activation barriers explaining that these solids are effective for the two synthesis [52]. Recent DFT calculations on the CH<sub>3</sub>OH decomposition and CO/H<sub>2</sub> reaction on Pt confirm these conclusions with additional data (a) the H<sub>2</sub> assisted CO dissociation leads to the preferential formation of OCH species as compared to COH species and (b) the C-O dissociation occurs at the level of the CH<sub>2</sub>O species forming adsorbed CH and OH species [53]. Finally, the existence of two reaction routes for the CH<sub>4</sub> formation from the CO/H<sub>2</sub> reaction on noble metal particles via adsorbed intermediates species of different reactivity, is consistent with the DFT calculations of Neurock [33] on Pd<sub>x</sub> clusters: in parallel to the most favorable route ( $\approx +75$  kJ/mol) via a migratory insertion of CO into a Pd-H bond to form formyl CHO there is a second reaction route via the coupling of H and CO over a bridge site which is less favorable (+130 kJ/mol) but may also occur under different conditions.

For the reorientation of the EMA of the CO/H<sub>2</sub> reaction on 2.9% Pt/Al<sub>2</sub>O<sub>3</sub> to obtain a theoretical rate of the CH<sub>4</sub> production at low

temperatures consistent with the experimental data, the different literature data [47–52] lead to the following comments (a) the accumulation of the methoxyl species during the CO/H<sub>2</sub> reaction before the H<sub>2</sub>-TPR [47–50] indicates that their production rate is faster than their consumption by hydrogenation/decomposition and (b) the hydrogenation of the methoxyl species being faster than that of the L CO species on Pt [47–50], this means that this adsorbed CO species is not the intermediate of the methoxyl formation (otherwise its coverage must be very low). Considering that the adsorption of CO on Pt sites is a necessary surface elementary step of any route for the CH<sub>4</sub> production, it comes that either the B or/and the 3FC CO species (inset Fig. 1) which represent a small fraction of the total amount of adsorbed CO at 300 K on the Pt particles (L CO is the dominant adsorbed species) must be implicated as adsorbed intermediate species for the CH<sub>4</sub> production at  $T < 520$  K (before the temperature at which the rate of hydrogenation of LCO species contributes to the CH<sub>4</sub> formation). The EMA has been reoriented by (a) considering that the B and/or the 3FC CO species are the active adsorbed CO species at low temperatures and (b) applying the Temkin-C and Temkin-C.R models developed for the L CO species to the two species. The heats of adsorption of the B and 3FC CO species at low and high coverages have been measured in a previous work using the AEIR method [5]: EB(0) = 94 kJ/mol, EB(1) = 45 kJ/mol, E3FC(0) = 135 kJ/mol and E3FC(1) = 104 kJ/mol. This allows a comparison of their coverages in the absence (curves a, b, c in Fig. 6A for the L, 3 FC and B CO species for 1% CO/He) and in the presence of hydrogen (curves d, e, f in Fig. 6A for the L, 3 FC and B CO species for 1% CO/H<sub>2</sub>) according to the Temkin and Temkin-C model [1] respectively. The calculations have been performed assuming that the heats of adsorption of hydrogen on the Pt sites adsorbing the B and 3FC CO species are the same that on the Pt sites adsorbing the L CO species. This assumption is justified by DFT calculations indicating that the heats of adsorption of hydrogen on different Pt sites are not strongly different [54–56] at the difference of the adsorption of H<sub>2</sub> on Ni and Pd sites [56].

Curve f in Fig. 6A indicates that the coverage of the B CO species is  $\approx 0$  at  $\approx 400$  K for 1% CO/H<sub>2</sub> due to the strong impact of the competitive chemisorption with H<sub>2</sub>: this adsorbed CO species cannot be the second route for the CH<sub>4</sub> production at  $T = 480$  K. Curve e in Fig. 6A shows that the coverage of the 3FC CO species remains high in the presence of 1% CO/H<sub>2</sub>:  $\theta_{3FC} = 0.997$  at 500 K and that this species can be envisaged as the intermediate species having a higher reactivity for hydrogen than the L CO species.

Note that curve f in Fig. 6A indicates that the coverage of the B CO species is of  $\approx 0.1$  at 300 K for 1% CO/H<sub>2</sub> showing that Pt sites are available for the hydrogen chemisorption whereas the coverages of the 3FC and L CO species are high. However, (a) this does not lead to the formation of CH<sub>4</sub> due to the high activation energy of step (4) and (b) it cannot be envisaged that adsorbed hydrogen species on the Pt sites liberated by the desorption of the B CO species contribute significantly to the hydrogenation of the L CO species otherwise this suppresses the competitive chemisorption between active adsorbed CO and hydrogen species leading to the CH<sub>4</sub> formation which has been demonstrated in numerous works [19,57].

Considering that the 3FC CO species is more reactive than the L CO species for the CH<sub>4</sub> production, calculations can be performed using the Temkin-C.R model to compare at low temperatures the experimental rate of the CH<sub>4</sub> production to a theoretical rate based on the adsorption/reactivity properties of the 3FC CO species. This comparison imposes the modification of the calculation of the experimental TOF (Eq. (27)) by using for Q<sub>Pt</sub> the amount of Pt sites adsorbing the 3FC species. This number has been estimated as follows: at the saturation of the sites at 300 K using 1% CO/H<sub>2</sub>, the IR band area of the L CO and 3FC CO species [1] are in the ratio  $\approx 6$ .

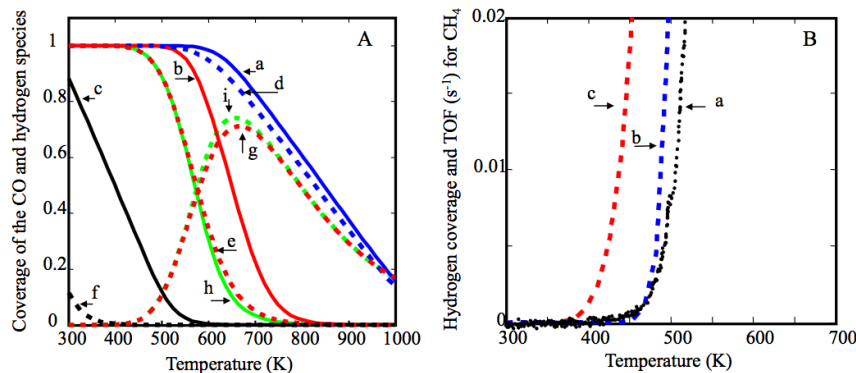


**Fig. 6.** EMA approach of the CO/H<sub>2</sub> reaction on 2.9% Pt/Al<sub>2</sub>O<sub>3</sub> based on the 3FC CO species as the adsorbed intermediate of the CH<sub>4</sub> formation at low temperatures. **Part A:** (a) (b) and (c) coverage of the L, 3FC and B CO species in the absence of competition with hydrogen using 1% CO/He (from Ref. [5]); (d) (e) and (f) coverage of the L, 3FC and B CO species during the competitive adsorption with hydrogen (without reaction) using 1% CO/H<sub>2</sub> considering the Temkin-C model; (g) coverage of the hydrogen species during the 1% CO/H<sub>2</sub> reaction considering the Temkin-C.R model; (h) and (i) coverages of the 3FC CO and hydrogen species during the 1% CO/H<sub>2</sub> reaction considering the Temkin-C.R model. **Part B:** (a) experimental rate of the CH<sub>4</sub> production for 1% CO/H<sub>2</sub>, (b) theoretical rate of the CH<sub>4</sub> production according to the Temkin-C.R model considering that the intermediate species is the 3FC CO species with an activation energy for the hydrogenation surface elementary step of  $E_r = 130$  kJ/mol; (c) coverage of the hydrogen species in competition with the 3FC CO species during the 1% CO/H<sub>2</sub> reaction according to the Temkin-C.R model.

Assuming similar infrared absorption coefficients for the two adsorbed species this indicates that  $Q_{Pt}$  for the 3FC CO species represents  $\approx 1/7$  of the total amount of adsorbed CO species at 300 K: this provides curve a in Fig. 6B. Considering that the kinetic mechanism for hydrogenation of the 3FC CO species to form CH<sub>4</sub> is similar to that of the L CO species, this allows us using the Temkin-C.R model developed for the L CO species with the heats of adsorption of the 3FC CO and hydrogen species (Table 1) and a new activation energy for hydrogenation of the 3FC CO species to obtain a theoretical rate of CH<sub>4</sub> production consistent with the experimental data. For instance curve b in Fig. 6B is obtained for  $E_r = 130$  kJ/mol, leading to curves h and i in Fig. 6A for the evolutions of the coverages of the 3FC CO and hydrogen species respectively. The curves are slightly different than those obtained by the Temkin-C model (curves e and g respectively) indicating that the Langmuir-Hinshelwood hydrogenation elementary step (4) does not disturb strongly the coverage of the two adsorbed species. Curve c in Fig. 6B shows that the coverage of the hydrogen species on the Pt sites forming the 3FC CO species starts to increase before the CH<sub>4</sub> production. Calculations performed with an activation energy of hydrogenation of  $E_r = 134$  kJ/mol for the 3FCO species leads to a theoretical rate of the CH<sub>4</sub> production consistent with the experimental data on a larger range of temperatures but with values lower than the experimental data at the beginning of the reaction (results not shown). Moreover, for  $E_r = 134$  kJ/mol the hydrogenation reaction does not disturb the competitive adsorption equilibrium of the 3FC CO and hydrogen species. Note that it is difficult in the present experimental conditions to perform an EMA based on the 3FC CO species, similarly to that describes for the L CO species, due to the low intensity of its IR band (inset Fig. 1). This can be envisaged by increasing significantly the weight of the catalyst pellet as performed for the measurement of the heats of adsorption of the 3FC and B CO species in the absence of hydrogen [5]. The fact that the 3FC and L CO species present different reactivity for hydrogen may explained the inflexion point observed at  $\approx 560$  K on the experimental rate of the CH<sub>4</sub> formation (Fig. 5): it corresponds to the beginning of the CH<sub>4</sub> production from the L CO species.

It appears from the present EMA that the CH<sub>4</sub> production from 1% CO/H<sub>2</sub> on 2.9% Pt/Al<sub>2</sub>O<sub>3</sub> is due to the hydrogenation of (a) the 3FC CO species for  $T < \approx 560$  K and (b) the 3FC and L CO species for  $T > \approx 560$  K. The involvement of the 3FC CO species as active species of the CH<sub>4</sub> production at low temperatures while they represent a small fraction of the total amount of adsorbed CO species is consistent with a conclusion of Vannice et al. [21] on the fact that

only a small fraction of the sites of the Pt particles are involved in the reaction. This is also consistent with the study of Tsai and Goodwin [58] on different metal supported catalysts in particular Pt/SiO<sub>2</sub> and Pt/C and dedicated to the comparison between (a) the total amount of adsorbed CO or hydrogen species (denoted N<sub>Chem</sub>) at low temperatures (300–373 K) and (b) the amount of active species (denoted N<sub>T</sub>) during the CO/H<sub>2</sub> reaction (H<sub>2</sub>/CO = 12, P<sub>T</sub> = 2.56 atm) at high temperatures (665 K) measured by steady-state isotopic transient kinetic analysis (SSITKA). On the Pt containing catalysts the ratio  $N_T^*/N_{Chem}$  is significantly lower than 1 ( $\approx 0.3$  and 0.1 on Pt/SiO<sub>2</sub> and Pt/C) indicating that the active CO species represents a fraction of the total amount of adsorbed CO at saturation of the Pt sites [58]. In the different interpretations of the low  $N_T^*/N_{Chem}$  ratio, the authors [58] consider that the adsorption equilibrium coverage of the main adsorbed CO species is decreased due to the high temperature of the reaction. However, this is not confirmed by calculations using the Temkin-C and the Temkin-C.R models with the parameters of Table 1 and using the experimental conditions of Tsai and Goodwin [58]: T = 665 K, P<sub>CO</sub> = (2.56/13) 10<sup>5</sup> Pa, P<sub>H2</sub> = (2.56 10<sup>5</sup> P<sub>CO</sub>) Pa: the coverage of the L CO species (which dominates the CO adsorption at 300 K) is of  $\approx 0.97$  without and with CH<sub>4</sub> production showing that the coverage is not significantly decreased in the experimental conditions of Ref. [58]. This means that the low  $N_T^*/N_{Chem}$  ratio measured by Tsai and Goodwin [58] is probably due to the fact that the active adsorbed CO species is not the dominant CO species quantified by N<sub>Chem</sub> (the L CO species) but the 3FCO species present in small amount on the Pt surface. Note that the estimated ratio between the 3FC and L CO species in the present study  $1/7 \approx 0.14$  is consistent with the  $N_T^*/N_{Chem}$  ratios of Tsai and Goodwin [58].

Finally the present EMA of the CO/H<sub>2</sub> reaction on 2.9% Pt/Al<sub>2</sub>O<sub>3</sub> leads to the conclusion that the dominant adsorbed L CO species cannot be considered as the adsorbed species having the highest reactivity for the CH<sub>4</sub> formation. It has been shown that this role must be ascribed to the 3FC CO species which represents a small fraction of the total amount of adsorbed CO species at 300 K. Other plausible kinetic models can be envisaged as support of a new EMA of the reaction. For instance, it can be suggested that there is non-competitive chemisorption between the active CO species and hydrogen. However, this is not consistent with (a) numerous literature data [19,57] and (b) the experimental evolution of the coverage of the L CO species before the CH<sub>4</sub> production which corresponds to the Temkin-C model (Fig. 2 and Part 1 [1]). Finally, it can be envisaged that the kinetic mechanism is more complex.

For instance it can be assumed that the CH<sub>4</sub> production is due to the overlap of two kinetic models: (a) a competitive adsorption between L CO and hydrogen as developed in the present study (active at  $T > 550$  K and allowing a consistent representation of the experimental evolutions of the coverage of the L CO and hydrogen species during a light-off test) overlapped at low temperatures ( $T$  in the range 485–540 K) with (b) a reaction between the L CO and the hydrogen species adsorbed on the Pt sites liberated by the decrease in the competitive adsorption equilibrium of the B CO species (Fig. 5). This last reaction may explain the formation of CH<sub>4</sub> at low temperatures from the L CO species without a significant modification of the coverage of the L CO species. Similarly, it can be envisaged as a development of the Temkin-C.R model that due to heterogeneity of the surface the activation energy of step (4) for the L CO species is dependent on its coverage for instance from 128 kJ/mol at high coverages (allowing to represent the evolution of the rate of the CH<sub>4</sub> production and the coverage (Fig. S1) at low temperatures: see Fig. S1 to a significant higher values at low coverages.

### 3.10. Comparison of the Temkin-C.R model to Langmuir models

Numerous kinetic studies on gas/solid catalytic reactions on heterogeneous surfaces are based on the Langmuir formalism. This situation is known as the “paradox of surface kinetics” [59] and different explanations have been proposed [59–61] whereas the kinetic parameters from this approach can be questionable [59]. In Part 1 [1], a comparison of the modelisation of the experimental data on the competitive CO-H<sub>2</sub> chemisorption on 2.9% Pt/Al<sub>2</sub>O<sub>3</sub> in the absence of reaction using either the Temkin or the Langmuir formalism has shown that (a) the competitive Langmuir model can be applied in short range of experimental conditions, (b) a competitive pseudo Langmuir model based on a mathematical approximation of the Langmuir model at a macroscopic level may lead to theoretical curves consistent with the experimental data for heats of adsorption different by  $\approx 20$ –30 kJ/mol than those obtained by the Temkin-C model. This comparison of the different models is developed in the present study by considering experimental conditions leading to the CH<sub>4</sub> production via the hydrogenation of the L CO species according to step (4). The Langmuir and pseudo Langmuir models for competitive adsorption with reaction (abbreviation Langmuir-C.R and pseudo Langmuir-C.R) consists solving Eqs. (11) and (12) in the temperature range (300–700 K by step of 1 K) considering that the heats of adsorption of the two adsorbed species are (a) either constant or (b) vary linearly with their coverages respectively as described in Part 1 [1] (Table 1) for the competitive chemisorption without reaction. Similarly to the Temkin-C.R model we consider for the pseudo Langmuir-C.R model that the activation energy of step (4) is independent on the coverage. In Table 1 the values of  $E_r$  are those leading to theoretical curves consistent as best as possible with the experimental data.

Curves a and b in Fig. 7 give the evolution of the coverages of the L CO and hydrogen species respectively with the reaction temperature from the Temkin-C.R model for 1% CO/H<sub>2</sub> (Table 1).

For the Langmuir-C.R model it is impossible to find a  $E_r$  value providing a theoretical coverage of the L CO species consistent with the experimental data in the range 300–713 K. Curves c and d in Fig. 7 give the coverages of the L CO and hydrogen species respectively according to this model using  $E_r = 120$  kJ/mol in Eqs. (11) and (12): curve c is consistent with the experimental data at the beginning of the decrease in the coverage of the L CO species. Curves c and d provide the theoretical rate of the CH<sub>4</sub> production (curve i in Fig. 7) consistent with the experimental data (curve g in Fig. 7) at low conversions. This means that from the Langmuir-C.R model it can be concluded from curves g and i that the L CO spe-

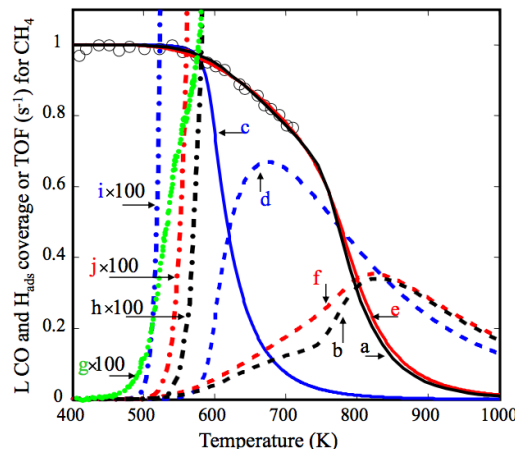


**Fig. 7.** Comparison of the experimental data recorded during the 1% CO/H<sub>2</sub> reaction on 2.9% Pt/Al<sub>2</sub>O<sub>3</sub> to different kinetic models. ○: experimental coverage of the L CO species; a and b [c and d] and [e and f] coverages of the L CO and hydrogen species from the Temkin-C.R [Langmuir] and [pseudo Langmuir-C.R] models; g experimental rate (TOF) of the CH<sub>4</sub> production, (h), (i) and (j) theoretical rate of the CH<sub>4</sub> production according to the Temkin-C.R, Langmuir-C.R. and pseudo Langmuir-C.R models respectively (see the text for more details).

cies is the intermediate of the CH<sub>4</sub> production. However, this is clearly related to the fact that this model does not take into account the experimental data revealing the heterogeneity of the surface such as the evolution of the coverage of L CO species in large ranges of experimental conditions (P<sub>CO</sub> and T, symbols ○). Similarly, the coverages of the L CO and hydrogen species according to the pseudo Langmuir-C.R model (curves e and f in Fig. 7) are obtained considering in Eqs. (11), (12) that the heats of adsorption of A and B linearly vary with their coverages as shown in Part 1 (Table 1) and selecting  $E_r = 144$  kJ/mol which provide a theoretical coverage of the L CO species almost overlapped with (a) the experimental data and (b) the theoretical coverage from the Temkin-C.R model. However, this  $E_r$  value provides a theoretical rate of the CH<sub>4</sub> production (curve j in Fig. 7) which is not consistent with the experimental data (curve g in Fig. 7) indicating similarly to the Temkin-C.R model that the L CO species cannot be the active adsorbed species at low temperatures. Finally, the pseudo Langmuir-C.R model based on a mathematical approximation which breaks the bases of the Langmuir model, appears are a reasonable approximation of the Temkin-C.R model but for a different set of kinetic parameters.

## 4. Conclusion

The present experimental microkinetic approach (EMA) of the CH<sub>4</sub> production from the CO hydrogenation using x% CO/H<sub>2</sub> ( $x = 1, 10^{-2}$  and  $10^{-3}$ ) on 2.9% Pt/Al<sub>2</sub>O<sub>3</sub> catalyst (Parts 1 and 2) clearly shows the interest of this procedure for the understanding of the surface elementary steps involved in the rate of the reaction. This procedure is distinct of a conventional kinetic study of catalytic reactions [62] which is mainly based on the interpretation of the experimental rate of the reaction via (a) a plausible detailed mechanism of the reaction and (b) Langmuir formalism associated with a series of simplifying assumptions. This provides a mathematical equation which is compared to the experimental data for the estimation of kinetic/thermodynamic parameters controlling the rate of the reaction. Conventionally, additional experimental data are presented to justify at least one of these parameters such as the heat of adsorption of a reactant using for instance microcalorimetry and/or TPD procedures. The first stage of an

EMA of a catalytic reaction is the characterization using conventional powdered catalysts of the kinetic/thermodynamic parameters of the surface elementary steps of a plausible kinetic model of the reaction. In a second stage, this allows the comparison of the experimental and theoretical rates of the reaction: an agreement validates the procedure whereas a discord imposes the modification of the kinetic model and the reorientation of the EMA. The EMA imposes to take into account the exact composition of the surface of the catalyst during the reaction in particularly the heterogeneity of the adsorption sites such as by (a) differentiating the role of the different adsorbed CO species in the catalytic reaction involving CO: i.e. Linear (L), Bridged (B) and three fold coordinated (3FC) CO species for CO/H<sub>2</sub> on Pt/Al<sub>2</sub>O<sub>3</sub> and (b) considering for each adsorbed species the intrinsic and/or induced heterogeneity of the adsorption sites.

The present study has been particularly dedicated to this last point and it is a contribution to the development of the EMA procedures. Previous studies have shown that the heats of adsorption of the L, B, 3FC CO species and the dissociated hydrogen species formed on 2.9% Pt/Al<sub>2</sub>O<sub>3</sub> in the absence of competition decrease linearly with their coverage according to the Temkin model [3–5,11]. This imposed considering how the competitive adsorption between the adsorbed hydrogen and CO species can be modeled via the Temkin formalism without (Part 1, model denoted Temkin-C) and with (Part 2, model denoted Temkin-C.R) a production of CH<sub>4</sub> at low and high temperatures respectively. To our knowledge, it is the first time that the Temkin formalism is exploited without simplifying mathematical approximations for the interpretation of a catalytic gas/solid reaction. For heterogeneous surface, we have shown the net advantages of this formalism compared to models based on the Langmuir formalism.

The characteristics and interests of the EMA are that large amounts of experimental data, obtained on the surface processes of a conventional catalyst, are taken into account to validate or to discard the plausible kinetic model selected for the interpretation of the rate of the catalytic reaction. For instance, for the CO/H<sub>2</sub> reaction on Pt/Al<sub>2</sub>O<sub>3</sub>, we have shown why the L CO species which is the dominant adsorbed CO species on Pt/Al<sub>2</sub>O<sub>3</sub> cannot be considered as the active species of the 1% CO/H<sub>2</sub> reaction at low temperature ( $T \approx 475$  K). This role has been ascribed to the 3FC CO species presents in small amount on the Pt particles.

The discrimination of the role of the different adsorbed CO species (and so of the different Pt sites) for the CO/H<sub>2</sub> reaction on Pt/Al<sub>2</sub>O<sub>3</sub> revealed by the accurate modeling of the experimental data from the Temlin-C.R model (coverages of the adsorbed CO and hydrogen species and rate of the CH<sub>4</sub> production) is consistent with previous studies [63,64] dedicated to the EMA of the CO/O<sub>2</sub> reaction on the same catalyst in the temperature range 300–500 K. In these conditions, it has been shown that the B CO species which is more weakly adsorbed than the L and 3FC CO species, liberates by desorption and oxidation, Pt sites for the adsorption of oxygen leading to the oxidation of the L and 3FC CO species which are strongly adsorbed. Clearly, the EMA shows that the diversity of the adsorbed species formed by a reactant such as CO on the surface of metal particles must be taken into account for the understanding of the surface elementary steps controlling the catalytic activity.

## Acknowledgments

Thanks are due to Dr. Paul Gravejat, for his contribution during the first stage of the calculations on the competitive chemisorption according to the Temkin formalism. D.B dedicates the present study to the memory of Stanislas Jean Teichner, former Professor at University of Lyon who passed away May 11, 2016 in Lyon, France. Named « Stany » or « Le Stan » by some of his international

and national colleagues and collaborators, he was a pioneer in different fields of heterogeneous catalysis such as photocatalysis, hydrogen spill over, synthesis of aerogel catalysts and in situ characterization of adsorbed species. It is on this last topic that he was my Ph.D. supervisor on the study by using IR spectroscopy of the adsorbed species formed on metal oxides during the isomerization of butenes. Later, as Assistant Professor, we have performed joint works in particular for the study of the adsorbed species during the methanol synthesis from CO/CO<sub>2</sub>/H<sub>2</sub> on zirconia containing metal oxides. I have strongly appreciated his enthusiasm to develop original research in heterogeneous catalysis and to encourage his young colleagues in this way.

## Appendix A. Supplementary material

Supplementary data associated with this article can be found, in the online version, at <http://dx.doi.org/10.1016/j.jcat.2017.05.013>.

## References

- [1] J. Couble, D. Bianchi, Experimental microkinetic approach of competitive chemisorption based on the Temkin model. 1. Case of CO and H<sub>2</sub> on 2.9 wt% Pt/Al<sub>2</sub>O<sub>3</sub>, *J. Catal.* 352 (2017) 672–685.
- [2] M.I. Temkin, The kinetics of some industrial heterogeneous catalytic reaction, *Adv. Catal.* 28 (1979) 173–291.
- [3] O. Dulaurent, D. Bianchi, Adsorption isobars for CO on a Pt/Al<sub>2</sub>O<sub>3</sub> catalyst at high temperatures using FTIR spectroscopy: isosteric heat of adsorption and adsorption model, *Appl. Catal. A* 196 (2000) 271–280.
- [4] A. Bourane, D. Bianchi, Heats of adsorption of the linear CO species on Pt/Al<sub>2</sub>O<sub>3</sub> using infrared spectroscopy: impact of the Pt dispersion, *J. Catal.* 218 (2003) 447–452.
- [5] A. Bourane, O. Dulaurent, D. Bianchi, Heats of adsorption of linear and multibound adsorbed CO species on a Pt/Al<sub>2</sub>O<sub>3</sub> catalyst using in situ infrared spectroscopy under adsorption equilibrium, *J. Catal.* 196 (2000) 115–125.
- [6] O. Dulaurent, K. Chandes, C. Bouly, D. Bianchi, Heat of adsorption of carbon monoxide on various Pt containing solids using in-situ infrared spectroscopy at high temperatures, *J. Catal.* 192 (2000) 273–285.
- [7] O. Dulaurent, A. Bourane, M. Nawaldi, D. Bianchi, Heat of adsorption of carbon monoxide on a Ru/Al<sub>2</sub>O<sub>3</sub> catalyst using adsorption equilibrium conditions, *J. Catal.* 201 (2000) 271–279.
- [8] S. Derrouiche, P. Gravejat, D. Bianchi, Heats of adsorption of linear CO species on the Au° and Ti+δ sites of a 1% Au/TiO<sub>2</sub> catalyst using in situ FTIR spectroscopy under adsorption equilibrium, *J. Am. Chem. Soc.* 126 (2004) 13010–13015.
- [9] J. Couble, D. Bianchi, Heat of adsorption of the linear CO species adsorbed on reduced Fe/Al<sub>2</sub>O<sub>3</sub> catalysts using the AEIR method in diffuse reflectance mode, *Appl. Catal. A* 409–410 (2011) 28–38.
- [10] J. Couple, D. Bianchi, Heats of adsorption of linearly adsorbed CO species on Co<sup>2+</sup> and Co<sup>0</sup> sites of reduced Co/Al<sub>2</sub>O<sub>3</sub> catalysts in relationship with the CO/H<sub>2</sub> reaction, *Appl. Catal. A* 445–446 (2012) 1–13.
- [11] S. Derrouiche, D. Bianchi, Heats of adsorption using temperature programmed adsorption equilibrium: application to the adsorption of CO on Cu/Al<sub>2</sub>O<sub>3</sub> and H<sub>2</sub> on Pt/Al<sub>2</sub>O<sub>3</sub>, *Langmuir* 20 (2004) 4489–4497.
- [12] T. Chafik, O. Dulaurent, J.L. Gass, D. Bianchi, Heat of adsorption of carbon monoxide on a Pt/Rh/CeO<sub>2</sub>/Al<sub>2</sub>O<sub>3</sub> three-way catalyst using in-situ infrared spectroscopy at high temperatures, *J. Catal.* 179 (1998) 503–514.
- [13] A. Bourane, O. Dulaurent, D. Bianchi, Comparison of the coverage of the linear CO species on Pt/Al<sub>2</sub>O<sub>3</sub> measured under adsorption equilibrium conditions by using FTIR, *J. Catal.* 195 (2000) 406–411.
- [14] S. Zeradine, A. Bourane, D. Bianchi, Comparison of the coverage of the linear CO species on Cu/Al<sub>2</sub>O<sub>3</sub> measured under adsorption equilibrium conditions by using FTIR and mass spectroscopy, *J. Phys. Chem. B* 105 (2001) 7254–7257.
- [15] A. Bourane, M. Nawaldi, D. Bianchi, Heats of adsorption of the linear CO species adsorbed on a Ir/Al<sub>2</sub>O<sub>3</sub> catalyst using in-situ FTIR spectroscopy under adsorption equilibrium, *J. Phys. Chem. B* 106 (2002) 2665–2671.
- [16] F. Giraud, C. Geantet, N. Guilhaume, S. Gros, L. Porcheron, M. Kanniche, D. Bianchi, Experimental microkinetic approach of De-NO<sub>x</sub> by NH<sub>3</sub> on V<sub>2</sub>O<sub>5</sub>/WO<sub>3</sub>/TiO<sub>2</sub> catalysts: Part 1—individual heats of adsorption of adsorbed NH<sub>3</sub> species on a sulfate-free TiO<sub>2</sub> support using adsorption isobars, *J. Phys. Chem. C* 118 (2014) 15664–15676.
- [17] M.A. Vannice, The catalytic synthesis of hydrocarbons from H<sub>2</sub>/CO mixtures over the group VIII Metals I. The specific activities and product distributions of supported metals, *J. Catal.* 31 (1975) 449–461.
- [18] M.A. Vannice, C.C. Twu, SMSI effects on CO adsorption and hydrogenation on Pt catalysts. Part II. Influence of support and crystallite size on the kinetics of methanation, *J. Catal.* 82 (1983) 213–222.
- [19] N.V. Pavlenko, N.I. Il'chenko, Y.I. Pyatnitskii, Kinetic and mechanistic features of carbon monoxide hydrogenation over supported transition metals, *Theor. Exp. Chem.* 33 (1997) 254–271.

- [20] P. Panagiotopoulou, D.I. Kondarides, X. Verykios, Selective methanation of CO over supported noble metal catalysts: effects of the nature of the metallic phase on catalytic performance, *Appl. Catal. A* 344 (2008) 45–54.
- [21] M.A. Vannice, C.C. Twu, S.H. Moon, SMSI effects on CO adsorption and hydrogenation on Pt catalysts. I. Infrared spectra of adsorbed CO prior to and during reaction conditions, *J. Catal.* 79 (1983) 70–80.
- [22] S. Shetty, A.P.J. Jansen, R.A. van Santen, Direct versus hydrogen-assisted CO dissociation, *J. Am. Chem. Soc.* 131 (2009) 12874–12875.
- [23] S. Shetty, R.A. van Santen, Hydrogen induced CO activation on open Ru and Co surfaces, *Phys. Chem. Chem. Phys.* 12 (2010) 6330–6332.
- [24] D.R. Alfonso, Further theoretical evidence for hydrogen-assisted CO dissociation, *J. Phys. Chem. C* 117 (2013) 20562–20571.
- [25] A. Anders Tuxen, S. Carencio, M. Chintapalli, C. Chuang, C. Escudero, E. Pach, P. Jiang, F. Borondics, B. Beberwyck, A.P. Alivisatos, G. Thornton, W. Pong, J. Guo, R. Perez, F. Besenbacher, M. Salmeron, Size-dependent dissociation of carbon monoxide on cobalt nanoparticles, *J. Am. Chem. Soc.* 135 (2013) 2273–2278.
- [26] P. van Helden, J. van den Berg, I.M. Ciobica, Hydrogen-assisted CO dissociation on the Co(211) stepped surface, *Catal. Sci. Technol.* 2 (2012) 491–494.
- [27] M. Ojeda, R. Nabar, A.U. Nilekar, A. Ishikawa, M. Mavrikakis, E. Iglesia, CO activation pathways and the mechanism of Fischer-Tropsch synthesis, *J. Catal.* 272 (2010) 287–297.
- [28] K. Yang, M. Zhang, Y. Yu, Direct versus hydrogen-assisted CO dissociation over stepped Ni and Ni<sub>3</sub>Fe surfaces: a computational investigation, *Phys. Chem. Chem. Phys.* 17 (2015) 29616–29627.
- [29] M.R. Elahifard, M.P. Jigato, J.W. Niemantsverdriet, Ab-initio calculations of the direct and hydrogen-assisted dissociation of CO on Fe(310), *Chem. Phys. Lett.* 534 (2012) 54–57.
- [30] S. Tada, R. Kikuchi, Mechanistic study and catalyst development for selective carbon monoxide methanation, *Catal. Sci. Technol.* 5 (2015) 3061–3070.
- [31] B. Miao, S.S.K. Ma, X. Wang, H. Su, S.H. Chan, Catalysis mechanisms of CO<sub>2</sub> and CO methanation, *Catal. Sci. Technol.* 6 (2016) 4048–4058.
- [32] S. Rönsch, J. Schneider, S. Matthischke, M. Schlüter, M. Götz, J. Lefebvre, P. Prabhakaran, S. Bajohr, Review on methanation – from fundamentals to current projects, *Fuel* 166 (2016) 276–296.
- [33] M. Neurock, First-principles analysis of the hydrogenation of carbon monoxide over palladium, *Top. Catal.* 9 (1999) 135–152.
- [34] M.A. Vannice, The catalytic synthesis of hydrocarbons from H<sub>2</sub>/CO mixtures over the group VIII Metals. II. The kinetics of the methanation reaction over supported metals, *J. Catal.* 37 (1975) 462–473.
- [35] J. Jagiellot, Stable numerical solution of the adsorption integral equation using splines, *Langmuir* 10 (1994) 2778–2785.
- [36] J.P. Prates Ramalho, G.V. Smirnov, On the structure of a local isotherm and solution to the adsorption integral equation, *Langmuir* 16 (2000) 1918–1923.
- [37] P. Szabelski, K. Nieszporek, Adsorption of gases on strongly heterogeneous surfaces. The integral equation approach and simulations, *J. Phys. Chem. B* 107 (2003) 12296–12302.
- [38] M. Primet, J.M. Basset, M.V. Mathieu, M. Prettre, Infrared investigation of hydrogen adsorption on alumina-supported platinum, *J. Catal.* 28 (1973) 368–375.
- [39] L.T. Dixon, R. Barth, J.W. Gryder, Infrared active species of hydrogen adsorbed by alumina-supported platinum, *J. Catal.* 37 (1975) 368–375.
- [40] J.P. Candy, P. Fouilloux, M. Primet, Adsorption d'Hydrogène entre 300 et 873 K sur un Catalyseur Pt/MgO, *Surf. Sci.* 72 (1978) 167–176.
- [41] R.J. Nichols, A. Bewick, Spectroscopic identification of the adsorbed intermediate in hydrogen evolution on platinum, *J. Electroanal. Chem.* 243 (1988) 445–453.
- [42] H. Ogasawara, M. Ito, Hydrogen adsorption on Pt(100), Pt(110), Pt(111) and Pt (1111) electrode surfaces studied by in situ infrared reflection absorption spectroscopy, *Chem. Phys. Lett.* 221 (1994) 213–218.
- [43] K. Kumimatsu, T. Senzaki, M. Tsushima, M. Osawa, A combined surface-enhanced infrared and electrochemical kinetics study of hydrogen adsorption and evolution on a Pt electrode, *Chem. Phys. Lett.* 401 (2005) 451–454.
- [44] K. Kumimatsu, T. Senzaki, G. Samjesk, M. Tsushima, M.A. Osawa, Hydrogen adsorption and hydrogen evolution reaction on a polycrystalline Pt electrode studied by surface-enhanced infrared absorption spectroscopy, *Electrochim. Acta* 52 (2007) 5715–5724.
- [45] P.R. Weisz, C.D. Prater, Interpretation of measurement in experimental catalysis, *Adv. Catal.* 6 (1954) 143–196.
- [46] A. Bourane, D. Bianchi, Oxidation of CO on a Pt/Al<sub>2</sub>O<sub>3</sub> catalyst: from the surface elementary steps to light-off tests V. Experimental and kinetic model for light-off tests in excess of O<sub>2</sub>, *J. Catal.* 222 (2004) 499–510.
- [47] J.L. Robbins, E. Marucchi-Soos, Evidence for multiple carbon monoxide hydrogenation pathways on platinum alumina, *J. Phys. Chem.* 93 (1989) 2885–2888.
- [48] T.F. Mao, J.L. Falconer, Methanation sites on a Pt/TiO<sub>2</sub> catalyst, *J. Catal.* 123 (1990) 443–455.
- [49] E. Hsiao, J.L. Falconer, Adsorption sites on Pd/Al<sub>2</sub>O<sub>3</sub>, *J. Catal.* 132 (1991) 145–156.
- [50] K.B. Kester, B. Chen, J.L. Falconer, Temperature-programmed methanation on Pd/La<sub>2</sub>O<sub>3</sub> and Pd/SiO<sub>2</sub> catalysts, *J. Catal.* 138 (1992) 294–305.
- [51] M.A. Vannice, Hydrogenation of CO and carbonyl functional groups, *Catal. Today* 12 (1992) 255–267.
- [52] E. Shustorovich, A.T. Bell, Analysis of CO hydrogenation pathways using the bond-order-conservation method, *J. Catal.* 113 (1988) 341–352.
- [53] R. Garcíá-Muelas, Q. Li, N. López, Density functional theory comparison of methanol decomposition and reverse reactions on metal surfaces, *ACS Catal.* 5 (2015) 1027–1036.
- [54] G. Paoletti, J.K. Nørskov, R. Hoffmann, A comparative theoretical study of the hydrogen, methyl, and ethyl chemisorption on the Pt(111) surface, *J. Am. Chem. Soc.* 122 (2000) 4129–4144.
- [55] G. Källén, G. Wahnström, Quantum treatment of H adsorbed on a Pt (111) surface, *Phys. Rev. B* 65 (2001) 033406–033410.
- [56] G.W. Watson, R.P.K. Wells, D.J. Willcock, G.J. Hutchings, A Comparison of the adsorption and diffusion of hydrogen on the {111}surfaces of Ni, Pd, and Pt from density functional theory calculations, *J. Phys. Chem. B* 105 (2001) 4889–4894.
- [57] R.E. Demmin, R.J. Gorte, A study of methanation kinetics on a clean and a titania-covered platinum foil, *J. Catal.* 105 (1987) 373–385.
- [58] Y.T. Tsai, J.G. Goodwin Jr., Comparison of chemisorption close to ambient vs. under reaction conditions for group VIII metal catalysts, *J. Catal.* 281 (2011) 128–136.
- [59] M. Boudart, Kinetics on ideal and real surfaces, *AIChE J.* 2 (1956) 62–64.
- [60] A. Corma, F. Llopis, J.B. Monton, S.W. Weller, Comparison of models in heterogeneous catalysis for ideal and non-ideal surfaces, *Chem. Eng. Sci.* 43 (1988) 785–792.
- [61] L.J. Broadbelt, J.E. Rekoske, Necessary levels of detail in microkinetic models of catalytic reaction on nonuniform surfaces, *Chem. Eng. Sci.* 51 (1996) 3337–3347.
- [62] G. Djéga-Mariadassou, M. Boudart, Classical kinetics of catalytic reactions, *J. Catal.* 216 (2003) 89–97.
- [63] A. Bourane, D. Bianchi, Oxidation of CO on a Pt/Al<sub>2</sub>O<sub>3</sub> catalyst: from the surface elementary steps to light-off tests: I. Kinetic study of the oxidation of the linear CO species, *J. Catal.* 202 (2001) 34–44.
- [64] A. Bourane, D. Bianchi, Oxidation of CO on a Pt/Al<sub>2</sub>O<sub>3</sub> catalyst: form the elementary steps to light-off tests. III. Experimental and kinetic model for lights-off tests in excess CO, *J. Catal.* 209 (2002) 126–134.

